

T-1879

FREQUENCY DOMAIN AND TIME DOMAIN SOLUTIONS
IN THE
MAGNETO-TELLURIC METHOD

by
Ulrich Schimschal
1977

ARTHUR LAKES LIBRARY
COLORADO SCHOOL of MINES
GOLDEN, COLORADO 80401

ProQuest Number: 10796119

All rights reserved

INFORMATION TO ALL USERS

The quality of this reproduction is dependent upon the quality of the copy submitted.

In the unlikely event that the author did not send a complete manuscript and there are missing pages, these will be noted. Also, if material had to be removed, a note will indicate the deletion.



ProQuest 10796119

Published by ProQuest LLC (2019). Copyright of the Dissertation is held by the Author.

All rights reserved.

This work is protected against unauthorized copying under Title 17, United States Code
Microform Edition © ProQuest LLC.

ProQuest LLC.
789 East Eisenhower Parkway
P.O. Box 1346
Ann Arbor, MI 48106 – 1346

T-1879

TO MY WIFE
SANDY
AND MY CHILDREN
TANYA
KARIN
JASON

ARTHUR LAKES LIBRARY
COLORADO SCHOOL of MINES
GOLDEN, COLORADO 80401

T-1879

A Thesis submitted to the Faculty and the Board of Trustees of the Colorado School of Mines in partial fulfillment of the requirements for the degree of Doctor of Philosophy in Geophysical Engineering.

Signed: Ulrich Schimschal
Ulrich Schimschal

Golden, Colorado

Date: March 31, 1977

Approved: George V. Keller
George V. Keller
Thesis Advisor

George V. Keller
George V. Keller
Head of Department

Golden, Colorado

Date: March 31, 1977

ABSTRACT

A controlled magneto-telluric depth-sounding technique is developed in the time domain by way of the theory of eigenfunctions. The use of Maxwell's equations leads to a differential equation that is solved by separation of variables. This in turn leads to an eigenvalue problem. Both harmonic and non-harmonic solutions are formulated in terms of eigenvalues.

The harmonic solution gives a result that is dependent on frequency. A computer program was developed for the multi-layered case of horizontal, isotropic, and homogeneous layers above an infinite half-space. Model curves of one and two layers above a half-space illustrate changes in resistivity, layer thickness, and permeability.

The nonharmonic solution results in an expression that gives the time derivative of the wave impedance as a function of time. A computer program was developed to evaluate the multi-layered case. Several graphs illustrate the functional behavior of this time dependent function. A comparison of time and frequency dependent solutions is made. Model curves are computed that include published values for the induced polarization effect.

The theoretical development shows that the rising slope portion of the wave impedance in the time domain contains the sought after information; i.e. layer thickness and

T-1879

resistivities of the geo-electric section. A controlled source magneto-telluric field technique is proposed that employs a single straight source wire of one-half to several kilometers in length, grounded by electrodes at each end, and utilizing a square current pulse as input into the ground. The receiver array would be placed at a distance of five times the source wire length. The measurement of the electric field would be accomplished by placing two straight wires, grounded by electrodes, at right angles to each other onto the earth's surface. The time rate of change of the magnetic field is to be measured by two horizontal induction coils placed at right angles to each other onto the surface of the ground.

The field data techniques as proposed above were not utilized; however, field data obtained from the "Long-Line Experiment" serve equally well to demonstrate the proposed theory. This experiment was conducted by sending current pulses of five minutes duration over a high voltage direct current transmission line. This power line extends from the Columbia River to Los Angeles. Data from this experiment demonstrate an example of the application of this new technique proposed in this work.

CONTENTS

	Page
ABSTRACT.....	iv
ILLUSTRATIONS	vii
ACKNOWLEDGMENTS	ix
TABLE OF SYMBOLS	x
INTRODUCTION.....	1
THEORY	3
DISCUSSION OF RESULTS	23
EVALUATION OF THE FIELD DATA	41
CONCLUSIONS	64
APPENDIX A	
Descriptions and listings of the computer programs	66
APPENDIX B	
Numerical results from field data evaluation and curve matching	84
REFERENCES	94

ILLUSTRATIONS

Figure	Page
1: Two-layer case, harmonic solution, apparent resistivities approach true resistivities	25
2: Three-layer case, harmonic solution, time periods are shown in seconds(s), minutes(m), hours(h), days(d)	26
3: Impedance over infinite half-space, nonharmonic solution	28
4: Two-layer case, comparison of harmonic vs. nonharmonic solution	30
5: Two-layer case, nonharmonic solution	31
6: Two-layer case, impedance vs. time	32
7: Model curves, time derivative of impedance vs. time, showing the effect of varying second layer resistivity	38
8: Model curves, time derivative of impedance vs. time, showing the effect of varying the parameter $\tau = \rho\epsilon$	39
9: Model curves, three-layer case, showing the effect of varying the layer thickness	40
9a: Survey location map	49
10: Station 4W, E-field, parallel component	50

11: Station 4W, E-field, perpendicular component	51
12: Station 4W, loop data, measuring the time rate of change of the vertical component of the magnetic field	52
13: Station 4W, impedance vs. time	53
14: Station 6W, E-field, parallel component	54
15: Station 6W, E-field, perpendicular component	55
16: Station 6W, loop data	56
17: Station 6W, impedance vs. time	57
18: Station 9W, E-field, parallel component	58
19: Station 9W, E-field, perpendicular component	59
20: Station 9W, loop data	60
21: Station 9W, impedance vs. time	61
22: Ratio of field data and half space	62
23: Station 9W, example of computer curve matching	63

ACKNOWLEDGEMENTS

The author wishes to express his appreciation to Dr. George V. Keller, who acted as thesis advisor, and to Dr. David Butler, Dr. Copeland, Dr. Martins, Dr. George R. Pickett, Dr. Robert J. Weimer for serving on my doctoral committee.

TABLE OF SYMBOLS

E_x, E_y, E_z	orthogonal Cartesian components of electric field vector \underline{E}
H_x, H_y, H_z	orthogonal components of magnetic field vector \underline{H}
$T(t)$	function of time in method of separation of variables
$Z(z)$	function of depth in method of separation of variables
λ	eigenvalue
ω	frequency in radians/second
σ	electrical conductivity
ρ	electrical resistivity
μ	magnetic permeability
ϵ	dielectric constant
h	layer thickness
$Z = \frac{E_x}{H_y}$	wave impedance
τ	$\rho\epsilon$
c	$1/\sqrt{\mu\epsilon}$
i	$\sqrt{-1}$
$T_t(t)$	$\frac{\partial T(t)}{\partial t}$
$T_{tt}(t)$	$\frac{\partial^2 T(t)}{\partial t^2}$
$Z_z(z)$	$\frac{\partial Z(z)}{\partial z}$
$Z_{zz}(z)$	$\frac{\partial^2 Z(z)}{\partial z^2}$

INTRODUCTION

The magneto-telluric depth-sounding method has seen infrequent use as an exploration tool. This is due in part to the difficulties associated with field data acquisition, and partly due to the difficulties inherent in the theoretical evaluation of the data.

The naturally occurring fluctuations of the earth's magnetic field are often quite weak, if not absent, and they may contain only a few dominant frequency components that can be measured. In order to construct a useful curve that can be matched to a conventional plot of apparent resistivities vs. a function of frequency it is necessary to have not only reliable amplitudes of both the E and H fields but also frequency components over several decades in width. To obtain representative amplitudes, field techniques have been developed where narrow bandpass filtering is employed. Computational transform techniques to obtain spectral amplitudes may give unreliable results. The motivation for this research was that a time dependent rather than frequency dependent theoretical result might perhaps be more useful for the evaluation of field data. One possible approach was that of simply computing a function in the time domain by the use of the Fourier transform. However, it was felt that the solution by the method of the separation of variables might

lead to a more practical result. The two equations resulting from the separation of variables were initially solved in terms of infinite power series to insure the most general solution. These power series were programmed and convergence was established. However, due to conceptual difficulties and programming expense the time dependent power series approach was later abandoned in favor of exponential solutions of the differential equations. This is the approach presented in this work.

Prior to this time no theory had been developed to evaluate magneto-telluric data in the time domain. The time domain solution is intended for application in controlled source magneto-tellurics. This technique eliminates problems encountered in detecting weak natural fields or difficulties encountered with recording during periods of low activity. Field techniques can be designed to insure that the theoretical assumptions of plane wave theory hold. Depth soundings may be taken at several locations using the same source. This in turn results in a more efficient field procedure compared to the more commonly used resistivity depth sounding techniques.

THEORY

In the magneto-telluric theory for plane waves the use of Maxwell's equations in conjunction with the appropriate constitutive relations results in the following equation (details of this derivation have been discussed by Keller and Frischknecht (1966)).

$$\nabla^2 \bar{E} = \frac{\mu}{\rho} \frac{\partial \bar{E}}{\partial t} + \epsilon \mu \frac{\partial^2 \bar{E}}{\partial t^2} \quad (1)$$

With the proper choice of coordinates equation (1) reduces to the single equation:

$$\frac{\partial^2 E_x}{\partial z^2} = \frac{\mu}{\rho} \frac{\partial \bar{E}_x}{\partial t} + \epsilon \mu \frac{\partial^2 E_x}{\partial t^2} \quad (2)$$

The solution to equation (2) making use of the method of separation of variables is as follows:

Let

$$E_x(z, t) = T(t) Z(z)$$

$$\frac{\partial^2 E_x}{\partial z^2} = T(t) z_{zz}(z)$$

$$\frac{\partial E_x}{\partial t} = T_t(t) z(z)$$

$$\frac{\partial^2 E_x}{\partial t^2} = T_{tt}(t) z(z)$$

Then

$$\frac{z_{zz}}{z} = \frac{\mu}{\rho} \frac{T_t}{T} + \epsilon\mu \frac{T_{tt}}{T}$$

Where $T_t = \frac{\partial T}{\partial t}$ and $z_{zz} = \frac{\partial^2 z}{\partial z^2}$

Then let

$$\frac{z_{zz}}{z} = -\lambda \quad (3a)$$

$$\epsilon\mu \frac{T_{tt}}{T} + \frac{\mu}{\rho} \frac{T_t}{T} = -\lambda \quad (3b)$$

Where λ is the eigenvalue common to both (3a) and (3b)

T-1879

Now let $Z(z)$ be represented by the infinite series:

$$Z(z) = b_0 + b_1 z + b_2 z^2 + \dots + b_n z^n + \dots \quad (4)$$

Rewriting (3a), we have

$$Z_{zz} + \lambda Z = 0 \quad (5)$$

The solution of (5) using (4) is:

$$Z(z) = b_0 \left(1 - \frac{\lambda z^2}{2!} + \frac{\lambda^2 z^4}{4!} + \dots + \frac{\lambda^n z^{2n}}{2n!} + \dots \right) + b_1 \left(z - \frac{\lambda z^3}{3!} + \dots + \frac{\lambda^n z^{2n+1}}{(2n+1)!} + \dots \right) \quad (6)$$

The quantities in parentheses above are the Taylor's series expansions of the sine and cosine functions; and the result is (see Churchill, 1963, p. 35) :

$$Z(z) = b_0 \cos \sqrt{\lambda} z + b_1 \sin \sqrt{\lambda} z \quad (7)$$

For negative values of λ , let us make the substitution

$\lambda = -m^2$ (m real); then equation (7) becomes:

$$Z(z) = b_0 \cos im z + b_1 \sin im z$$

$$\begin{aligned}
 &= b_0 \cosh m z + i b_1 \sinh m z \\
 &= \left(\frac{b_0 + i b_1}{2} \right) e^{mz} + \left(\frac{b_0 - i b_1}{2} \right) e^{-mz} \\
 &= B \cosh (mz + \gamma) \quad (8)
 \end{aligned}$$

Where $B = \sqrt{b_0^2 + b_1^2}$

and $\gamma = \ln \sqrt{\frac{b_0^2 - b_1^2 + i 2b_0 b_1}{b_0^2 + b_1^2}}$

For equation (3b) we have

$$\epsilon \mu T_{tt} + \frac{\mu}{\rho} T_t + \lambda T = 0$$

Rewriting

$$T_{tt} + \frac{1}{\rho \epsilon} T_t + \frac{\lambda}{\mu \epsilon} T = 0$$

To simplify notation let:

$$\rho \epsilon = \tau \quad \text{and} \quad \frac{1}{\mu \epsilon} = c^2$$

T-1879

We get

$$T_{tt} + \frac{1}{r} T_t + \lambda c^2 T = 0 \quad (10)$$

Or, generally

$$T_{tt} + p_1 T_t + p_2 T = 0 \quad (11)$$

Equation (11), however, is one of the more common differential equations used in mechanics, electricity, etc. The discussion that follows is essentially the one given by Bear (1962).

The solution of equation (11) is:

$$e^{rt} (r^2 + p_1 r + p_2) \quad (12)$$

Where

$$r^2 + p_1 r + p_2 = 0 \quad (13)$$

is the auxiliary equation for (12)

From (10) we get:

T-1879

$$r^2 + \frac{1}{\tau} r + \lambda c^2 = 0 \quad (14)$$

The solutions to equation (14) are:

$$r_{1,2} = -\frac{1}{2\tau} \pm \sqrt{\frac{1}{4\tau^2} - \lambda c^2} \quad (15)$$

Or finally, for $\frac{1}{4\tau^2} < \lambda c^2$

$$T(t) = e^{\frac{-t}{2\tau}} \left(a_0 \cos \sqrt{\lambda c^2 - \frac{1}{4\tau^2}} t + a_1 \sin \sqrt{\lambda c^2 - \frac{1}{4\tau^2}} t \right) \quad (16)$$

Or, equivalent to (16)

$$T(t) = A e^{\frac{-t}{2\tau}} \sin(\omega t + \alpha) \quad (17)$$

$$\text{where } \omega = \sqrt{\lambda c^2 - \frac{1}{4\tau^2}} \quad (18)$$

i.e., ω is a function of the eigenvalue λ . For negative values of λ , as before, let $\lambda = -m^2$; the solution to equation (10) becomes:

T-1879

$$T(t) = e^{\frac{-t}{2\tau}} \left(a_0 e^{ut} + a_1 e^{-ut} \right) \tag{19}$$

Where
$$u = \sqrt{\frac{1}{4\tau^2} + m^2 c^2} \tag{20}$$

Equation (19) can be rewritten (see Keller and Frischknecht, 1966)

$$T(t) = 2e^{\frac{-t}{2\tau}} \sqrt{a_0 a_1} \cosh \left(ut + \ln \sqrt{\frac{a_0}{a_1}} \right) \tag{21}$$

Next we need to compute the wave impedance Z, defined as

$$Z = \frac{E_x}{H_y}$$

The approach that follows is borrowed from Keller and Frischknecht, 1966, p. 215.

$$E_x = T(t) Z(z) \quad ; \quad \frac{\partial E_x}{\partial z} = T(t) Z_z(z)$$

$$H_y = H_{y,o} T(t) \quad ; \quad \frac{\partial H_y}{\partial t} = H_{y,o} T_t(t)$$

$$H_{y,o} = \frac{H_y}{T(t)} \quad ; \quad \frac{\partial H_y}{\partial t} = \frac{T_t(t)}{T(t)} H_y \quad (22)$$

and from

$$\frac{\partial E_x}{\partial z} = -\mu \frac{\partial H_y}{\partial t}$$

$$T(t) Z_z(z) = -\mu \frac{T_t(t)}{T(t)} H_y$$

$$\text{or } H_y = \frac{-T^2(t)}{\mu T_t(t)} Z_z(z) \quad (23)$$

T-1879

$$\text{Then } z = \frac{Ex}{Hy} = -u \frac{T_t(t)}{T(t)} \frac{Z(z)}{Z_z(z)} \quad (24)$$

Next we need to evaluate the expression:

$$\frac{T_t(t)}{T(t)} \quad (\text{See equation (24)})$$

We will first derive this expression for equation (21),

i.e.,

$$T(t) = 2e^{\frac{-t}{2\tau}} \sqrt{a_0 a_1} \cosh \left(ut + \ln \sqrt{\frac{a_0}{a_1}} \right)$$

From (21) we get for $T_t(t)$

$$T_t(t) = 2\sqrt{a_0 a_1} e^{\frac{-t}{2\tau}} \left[\frac{-1}{2\tau} \cosh(ut + \beta) + u \sinh(ut + \beta) \right] \quad (25)$$

$$\text{where } \beta = \ln \sqrt{\frac{a_0}{a_1}}$$

Equation (25) can be simplified by the following manipulations:

Let a be a number such that

$$a = \sqrt{u^2 - \left(\frac{1}{2\tau}\right)^2}$$

T-1879

or

$$a^2 = u^2 - \left(\frac{1}{2\tau}\right)^2 \quad (26)$$

Dividing by a

$$1 = \left(\frac{u}{a}\right)^2 - \left(\frac{1}{2\tau a}\right)^2 \quad (27)$$

Equation (27) is seen to have the form

$$\cosh^2 x - \sinh^2 x = 1$$

Equation (27) holds for an arbitrary a , let a be chosen such that

$$\cosh \beta = \frac{u}{a}$$

$$\sinh \beta = \frac{1}{2\tau a} \quad (28)$$

However

$$\cosh (x - y) = \cosh x \cosh y - \sinh x \sinh y$$

Finally we have from (21)

(29)

T-1879

$$\begin{aligned}
T_t &= -2 \sqrt{a_0 a_1} e^{\frac{-t}{2\tau}} a \left[\frac{1}{a} \cosh (u t + \beta) - \frac{u}{a} \sinh (u t + \beta) \right] \\
&= 2 \sqrt{a_0 a_1} e^{\frac{-t}{2\tau}} a \left[\cosh \beta \cosh (u t + \beta) - \sinh \beta \sinh (u t + \beta) \right] \\
&= -2 \sqrt{a_0 a_1} e^{\frac{-t}{2\tau}} a \sinh (-u t) \quad (30)
\end{aligned}$$

Or

$$T_t(t) = 2 \sqrt{a_0 a_1} e^{\frac{-t}{2\tau}} a \sinh u t \quad (31)$$

Dividing by (21)

$$\frac{T_t(t)}{T(t)} = \frac{a \sinh u t}{\cosh (u t + \beta)} \quad (32)$$

$$\text{where } a = \sqrt{u^2 - \frac{1}{4\tau^2}} = mc$$

$$\text{and } \beta = \tanh^{-1} \frac{1}{2\tau u} = \tanh^{-1} \frac{1}{\sqrt{1 + 4\tau^2 m^2 c^2}}$$

$$u = \sqrt{\frac{1}{4\tau^2} + m^2 c^2}$$

T-1879

Using a similar approach (see Bear, 1962) as before with equation (17), i.e.,

$$T(t) = Ae^{\frac{-t}{2\tau}} \sin(\omega t + \alpha)$$

we get

$$\frac{T_t}{T} = \frac{\sqrt{\omega^2 + \frac{1}{4\tau^2}} \sin \omega t}{\sin(\omega t + \alpha)} \quad (33)$$

where $\alpha = \tan^{-1} 2\omega\tau$

Equation (24) can now be treated similarly to the approach used in Keller and Fris chknecht, 1966, p.216.

To simplify matters the following notation will be used;

let:

$$B^{(j)} = -\mu^{(j)} \frac{T_t(\lambda, t, \rho^{(j)}, \epsilon^{(j)}, \mu^{(j)})}{T(\lambda, t, \rho^{(j)}, \epsilon^{(j)}, \mu^{(j)})} \quad (34)$$

and $Z_i^{(j)}$ = wave impedance in layer (j) at depth z_i

also from (7)

T-1879

$$z_z(z) = \left[-b_0 \sin \sqrt{\lambda} z + b_1 \cos \sqrt{\lambda} z \right] \sqrt{\lambda} \quad (35)$$

Then (24) becomes

$$z_i^{(j)} = \frac{B^{(j)}}{\sqrt{\lambda}} \frac{b_0 \cos \sqrt{\lambda} z_i + b_1 \sin \sqrt{\lambda} z_i}{-b_0 \sin \sqrt{\lambda} z_i + b_1 \cos \sqrt{\lambda} z_i} \quad (36)$$

$$z_{i+1}^{(j)} = \frac{B^{(j)}}{\sqrt{\lambda}} \frac{b_0 \cos \sqrt{\lambda} z_{i+1} + b_1 \sin \sqrt{\lambda} z_{i+1}}{-b_0 \sin \sqrt{\lambda} z_{i+1} + b_1 \cos \sqrt{\lambda} z_{i+1}} \quad (37)$$

$$\text{Then } \frac{b_0}{b_1} = \frac{z_{i+1}^{(j)} \sqrt{\lambda} - B^{(j)} \tan \sqrt{\lambda} z_{i+1}}{B^j + \sqrt{\lambda} \tan \sqrt{\lambda} z_{i+1} z_{i+1}^{(j)}} \quad (38)$$

Finally eliminating $\frac{b_0}{b_1}$

$$z_i^{(j)} = \frac{B^{(j)}}{\sqrt{\lambda}} \frac{\left[z_{i+1}^{(j)} \sqrt{\lambda} + B^j \tan \sqrt{\lambda} (z_i - z_{i+1}) \right]}{\left[-z_{i+1}^{(j)} \sqrt{\lambda} \tan \sqrt{\lambda} (z_i - z_{i+1}) + B^{(j)} \right]} \quad (39)$$

For reasons that will become apparent shortly the eigenvalues are now restricted to $=-m^2$, Then (39) becomes:

T-1879

$$Z_i^{(j)} = \frac{B^{(j)}}{m} \left[\frac{Z_{i+1}^{(j)} m + B^{(j)} \tanh m(z_i - z_{i+1})}{m Z_{i+1}^{(j)} \tanh m(z_i - z_{i+1}) + B^{(j)}} \right] \quad (40)$$

For the semi-infinite halfspace we get from (40) at z_0 ,

i.e. $z=0$

$$Z_0^{(1)} = \frac{B^{(1)}}{m} \left[\frac{Z_\infty^{(1)} m - B^{(1)} \tanh m z_\infty}{-Z_\infty^{(1)} m \tanh m z_\infty + B^{(1)}} \right] \quad (41)$$

But $\lim_{z \rightarrow \infty} \tanh mz = 1$ for a given m (42)

$$Z_0^{(1)} = \frac{-B^{(1)}}{m} \left[\frac{Z_\infty^{(1)} m - B^{(1)}}{Z_\infty^{(1)} m - B^{(1)}} \right] = -\frac{B^{(1)}}{m} = \frac{\mu}{m} \frac{T_t(t)}{T(t)} \quad (43)$$

The restriction of $\lambda = -m^2$, necessary to obtain a solution to equation (40), using (42), makes it necessary that equation (32) is used in the solution of the wave impedance (see Churchill, 1963). Combining equations (32) and (43) we obtain for the impedance at the surface of a semi-infinite halfspace using (32):

T-1879

$$z_0^{(1)} = \mu c \frac{\sinh ut}{\cosh (ut + \beta)} = \sqrt{\frac{\mu}{\epsilon}} \frac{\sinh ut}{\cosh (ut + \beta)} \quad (44)$$

$$\text{Where } u = \sqrt{\frac{1}{4\tau^2} + m^2 c^2}$$

$$\text{And } \beta = \tanh^{-1} \frac{1}{2\tau u}$$

For the two-layer case, i.e. one layer above a semi-infinite halfspace, we have from (40) and (41)

$$z_1^{(2)} = -\frac{B^{(2)}}{m}$$

$$z_0^{(1)} = \frac{B^{(1)}}{m} \frac{\left[z_1^{(1)} m + B^{(1)} \tanh m (z_0 - z_1) \right]}{\left[m z_1^{(1)} \tanh m (z_0 - z_1) + B^{(1)} \right]}$$

At $z = z_1$ we have the boundary condition $z_1^{(2)} = z_1^{(1)}$; hence

$$z_0^{(1)} = \frac{B^{(1)}}{m} \frac{\left[-B^{(2)} + B^{(1)} \tanh m (-z_1) \right]}{\left[-B^{(2)} \tanh m (-z_1) + B^{(1)} \right]} \quad \text{Where } z_0 = 0$$

By comparison for the harmonic solution of equation (10),

let

T-1879

$$T(t) = e^{i\omega t}, \quad \text{Then from (10)} \quad (45)$$

$$\omega^2 - \frac{i\omega}{\tau} - \lambda c^2 = 0 \quad (46)$$

$$\omega_{1,2} = \frac{i}{2\tau} \pm \sqrt{\frac{-1}{4\tau^2} + \lambda c^2} = i \left(\frac{1}{2\tau} \pm \sqrt{\frac{1}{4\tau^2} + m^2 c^2} \right)$$

or

$$i\omega_{1,2} = -\frac{1}{2\tau} \pm \sqrt{\frac{1}{4\tau^2} + m^2 c^2} \quad (47)$$

From equation (19) we have for comparison

$$T(t) = a_0 \text{EXP} \left[\left(\frac{-1}{2\tau} + \sqrt{\frac{1}{4\tau^2} + m^2 c^2} \right) t \right] + a_1 \text{EXP} \left[\left(\frac{-1}{2\tau} - \sqrt{\frac{1}{4\tau^2} + m^2 c^2} \right) t \right] \quad (48)$$

From (46) we get for m^2

$$m^2 = \left(\frac{-\omega^2}{c^2} + \frac{i\omega}{\tau c^2} \right)$$

or

$$m^2 = \left(\frac{i\omega\mu}{\rho} - \omega^2 \mu\epsilon \right) \quad (49)$$

T-1879

For a third type of solution (see Stratton, 1941), let

$$m = iq \text{ (q real), i.e., } \lambda = q^2$$

We get from (14)

$$r^2 + \frac{1}{\tau} r + q^2 c^2 = 0$$

and from (16)

$$T(t) = e^{\frac{-t}{2\tau}} \left(a_0 \cos \sqrt{q^2 c^2 - \frac{1}{4\tau^2}} t + a_1 \sin \sqrt{q^2 c^2 - \frac{1}{4\tau^2}} t \right)$$

For $\frac{1}{4\tau^2} < q^2 c^2$ we get from (33)

$$\frac{T_t}{T} = \sqrt{\omega^2 + \frac{1}{4\tau^2}} \frac{\sin \omega t}{\sin(\omega t + \alpha)} \quad (50)$$

where $\omega = \sqrt{q^2 c^2 - \frac{1}{4\tau^2}}$ and $\alpha = \tan^{-1} 2\omega\tau$

$$\text{Or } \frac{T}{T_t} = qc \frac{\sin \omega t}{\sin(\omega t + \alpha)} \quad (51)$$

In both equations (51) and (32) we have time dependence of the impedance. The frequency is a function of the separation constant.

T-1879

In the latter case equation (39) becomes applicable, i.e.

$$z_i^{(j)} = \frac{B^{(j)}}{q} \frac{\left[z_{i+1}^{(j)} q + B^{(j)} \tan q (z_i - z_{i+1}) \right]}{\left[-z_{i+1}^{(j)} q \tan q (z_i - z_{i+1}) + B^{(j)} \right]} \quad (52)$$

T-1879

We will now modify the assumption made on page 10 (equation 22). From (22) and (23) we have:

$$\frac{\partial H}{\partial t} = -\frac{1}{\mu} T(t) Z_z(z)$$

$$\text{Let } T^t = \int T(t) dt$$

$$\text{Then } H = -\frac{1}{\mu} T^t(t) Z_z(z)$$

$$\text{and } \frac{E_x}{H_y} = -\mu \frac{T}{T^t} \frac{Z}{Z_t}$$

(53)

From (19) we have

$$T(t) = a_0 e^{(-\frac{1}{2\tau} + u)t} + a_1 e^{-(\frac{1}{2\tau} + u)t}$$

or

$$T^t = e^{-\frac{t}{2\tau}} \left\{ \frac{a_0}{-\frac{1}{2\tau} + u} e^{ut} + \frac{a_1}{-\frac{1}{2\tau} - u} e^{-ut} \right\}$$

We now introduce the condition that $E_x(z, t)$ at $t=0$ is zero, i.e.

$$E_x(z, 0) = 0$$

This requires that the constant $a_1 = -a_0$, or

$$\frac{T(t)}{T^t(t)} = \frac{e^{ut} - e^{-ut}}{e^{ut} + e^{-ut}} \cdot \frac{-\frac{1}{2\tau} + u}{\frac{1}{2\tau} + u}$$

T-1879

Simplifying we get:

$$\frac{T(t)}{T'(t)} = \frac{e^{ut} - e^{-ut}}{\frac{2\tau(2\tau u + 1)}{4\tau^2 u^2 - 1} e^{ut} + \frac{2\tau(2\tau - 1)}{4\tau^2 u^2 - 1} e^{-ut}}$$

$$= \frac{2 \sinh ut (4\tau^2 u^2 - 1)}{2\tau[(2\tau u + 1) e^{ut} + (2\tau u - 1) e^{-ut}]}$$

which, using (55)

$$= \frac{2\tau^2 m^2 c^2 \tanh ut}{2\tau^2 u + \tanh ut}$$

or, simplifying

$$= \frac{2\tau^2 m^2 c^2 \tanh ut}{\tau \sqrt{1 + 4\tau^2 m^2 c^2} + \tanh ut}$$

(54)

$$\text{where } u^2 = \frac{1}{4\tau} + m^2 c^2$$

(55)

DISCUSSION OF THE RESULTS

A computer program was written for the n-layered case utilizing equation (40). For the harmonic case equations (45) and (49) were used in connection with equation (40); the variable ω being independent. For the nonharmonic case equation (32) is used with equation (40); the variable m being independent. In the discussion below the results of the harmonic solution are discussed first; followed by the results from the nonharmonic solution.

Harmonic solution

In programming the harmonic case the long-wavelength approximation was not utilized. This prevents erroneous values at high frequencies. We have for the impedance ($Z_0^{(1)}$) at the surface of an infinite halfspace:

$$Z_0^{(1)} = \frac{\mu i \omega}{m} = \frac{i \mu \omega}{(i \omega \mu \sigma - \mu \epsilon \omega^2)^{1/2}} = \left(\frac{i \mu \omega}{\sigma + i \epsilon \omega} \right)^{1/2} \quad (53)$$

Solving for ρ , the definition for the apparent resistivity ρ_A becomes:

$$\rho_A = \frac{i Z^2}{\omega (\epsilon Z^2 - \mu)} \quad (54)$$

Equation (53) shows that for high frequencies the impedance will approach the constant $(\mu/\epsilon)^{1/2}$. The results of a two-layer case are shown in Figure 1. It was plotted in a conventional way

$$\rho_A/\rho_1 \text{ vs. } \frac{1}{h_1 \gamma_1} \text{ where } h_1$$

represents the thickness of the first layer, and m_1 is a function of the first-layer parameters. The log-log plot shows the usual symmetry obtained in this type of plot. Published curves make the assumption of infinitely conductive or resistive basement resulting in 45° slopes at low frequencies. A three-layer case is shown in Figure 2. Again it was plotted in a conventional manner. The corresponding periods are shown in seconds (s), minutes (m), hours (h), and days (d). For long enough periods it can be seen that just like in the two-layer case the curves will approach the resistivities of the underlying halfspace. Included for comparison Figure 2 furthermore contains an example of a change in permeability for the second layer. The permeability used here is that representative of a basalt.

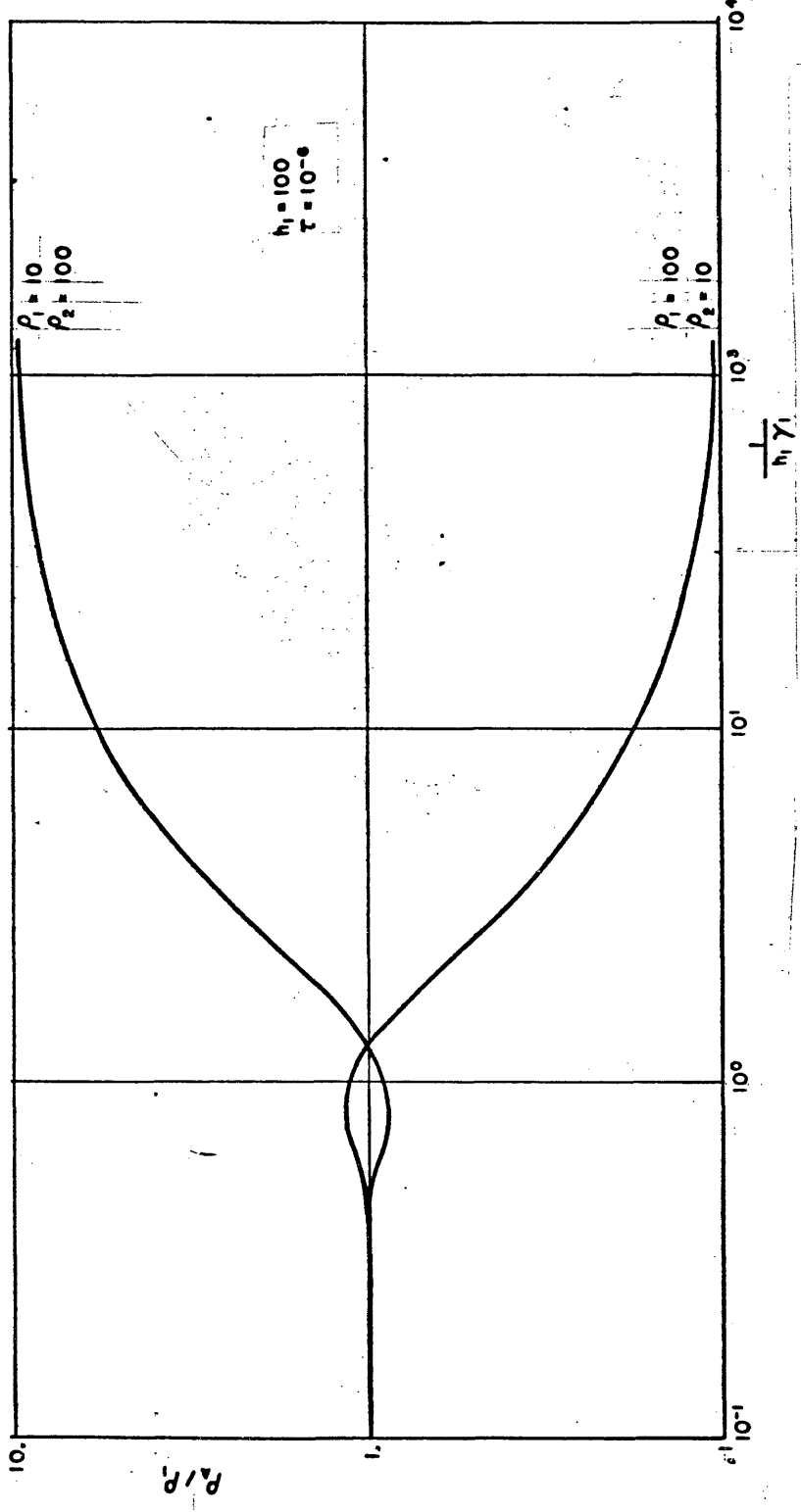


Figure 1: Two-layer case, harmonic solution, apparent resistivities approach true resistivities

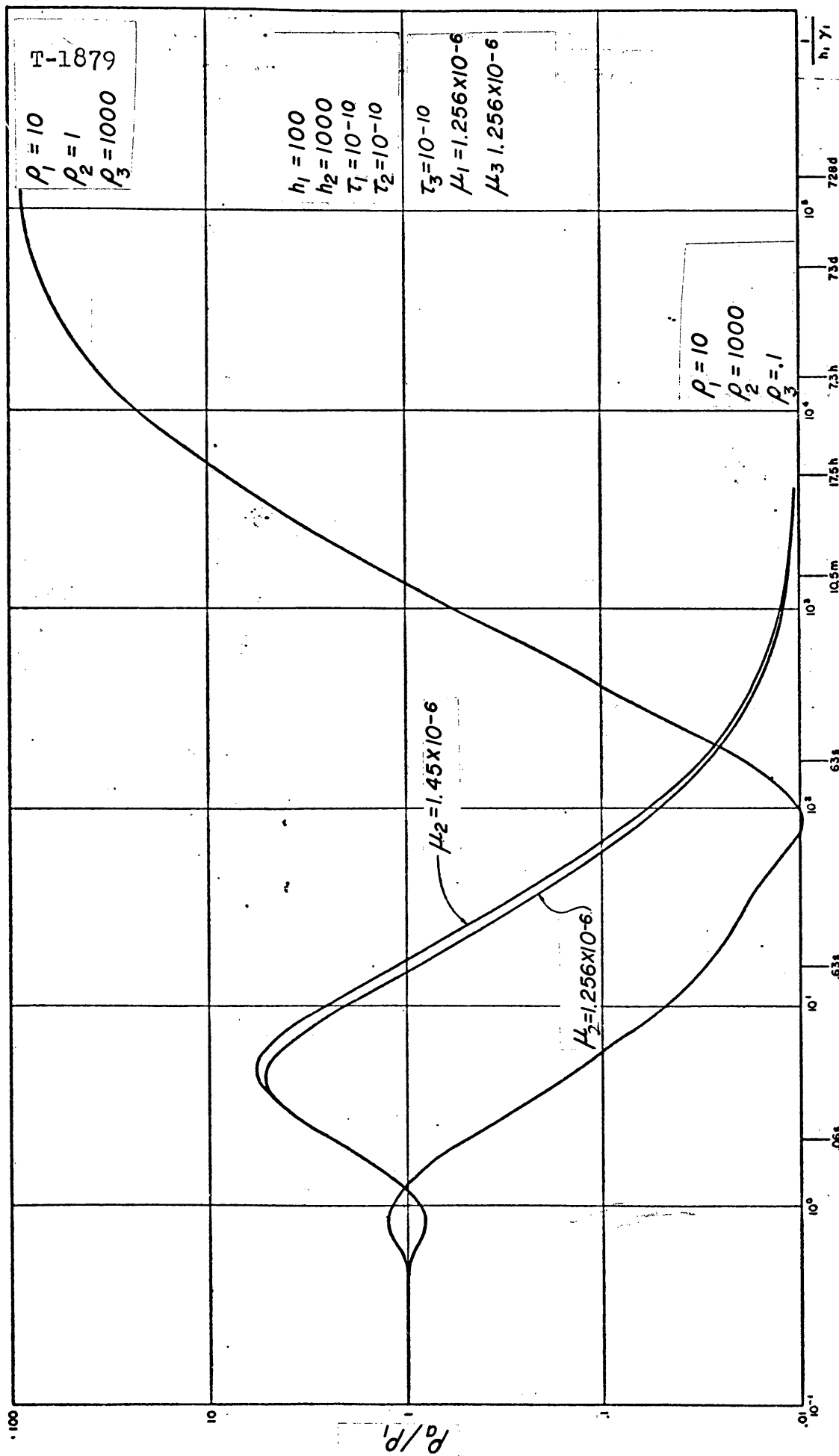


Figure 2: Three-layer case, harmonic solution, time periods are shown in seconds(s), minutes(m), hours(h), and days(d)

Nonharmonic solution

The nonharmonic solution is illustrated in Figures 3, 4, 5, and 6. There is no easily definable quantity like an apparent resistivity for this type of solution. The input to the computer program was written in terms of ρ , μ , and τ , where $\tau = \rho\epsilon$. The constant ϵ represents an apparent dielectric constant. Representative values of τ were obtained from the table on p.463, Keller and Frischknecht, 1966. Figure 3 shows (equation (44)) the impedance $Z_0^{(1)}$ at the surface of an infinite halfspace plotted vs. the eigenvalue m . For large values of m the impedance goes to the constant $\sqrt{\mu/\epsilon}$. This is the same value attained for high frequencies in the case of the harmonic solution. For small values of m the impedance goes to zero. For a given value of m the impedance attains a maximum value generally for values of t greater than 1.0. Hence for large enough values of t the impedance becomes a function of m only. This is also illustrated on Figure 3.

In order to compare the harmonic and nonharmonic solutions Figure 4 was included. Curve A is the upper curve on Figure 1 replotted in terms of $Z_0^{(1)}/\sqrt{\mu/\epsilon}$ vs. period T . Curve B shows the solution for the nonharmonic case. The latter was plotted against $T^{(1)}$, where:

$$T^{(1)} = \frac{2\pi}{|\omega_1|} \quad (\text{see equation (47)})$$

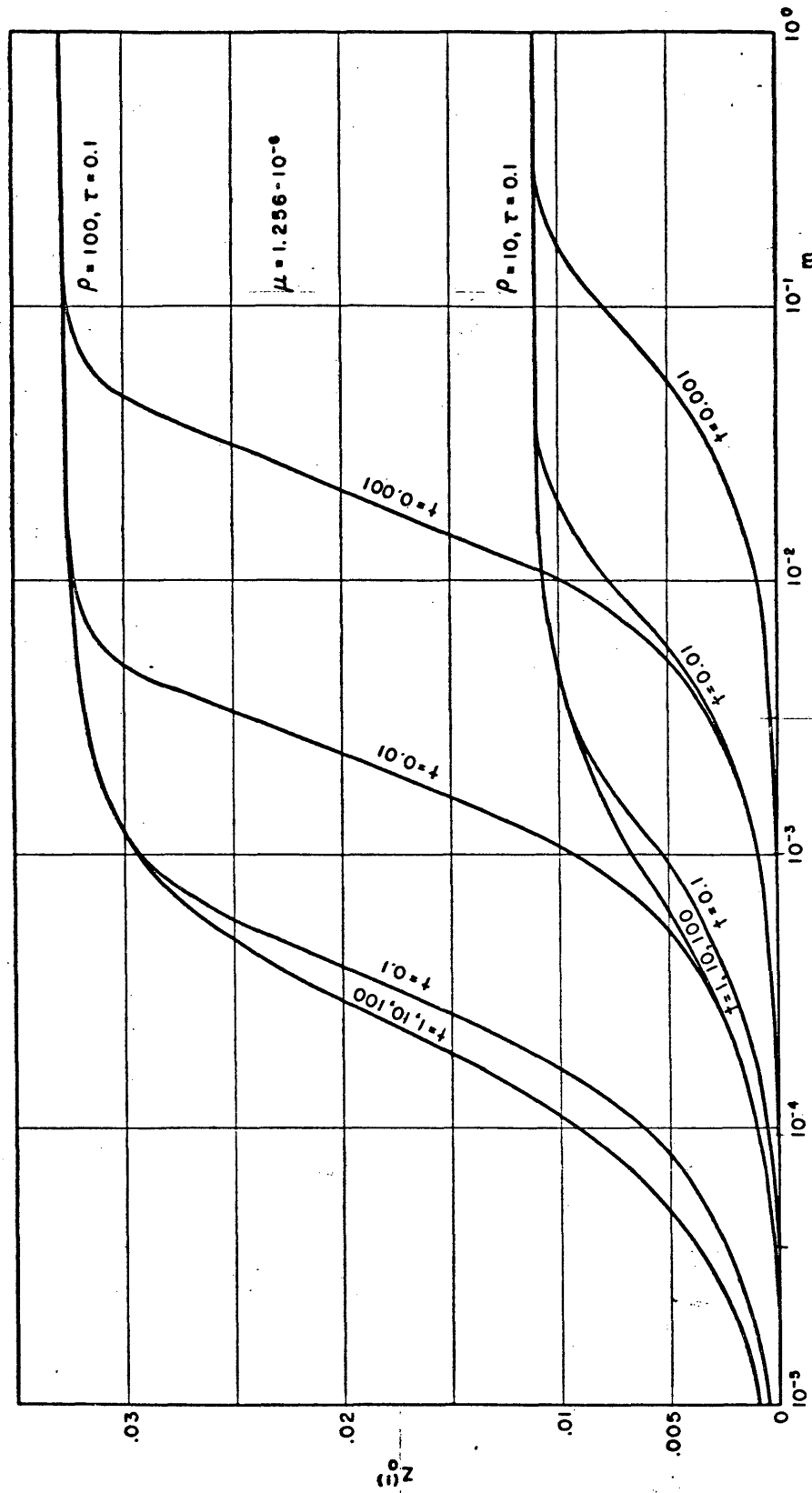


Figure 3: Impedance over infinite half-space, nonharmonic solution

and

$$\tau = \rho^{(1)} \epsilon^{(1)}, c = \frac{1}{\sqrt{\mu^{(1)} \epsilon^{(1)}}}$$

Figure 5 was included to illustrate a two-layer case for large values of t and two different layer thicknesses.

To obtain a solution of the impedance vs. time the function for a two-layer case was integrated over a range of the eigenvalue m . The eigenvalue m is a continuous variable. However, the summation of eigenfunctions over some given range is also a solution of the original differential equation. The problem is one of synthesizing a time function from a suitable range of eigenfunctions. Figure 6 shows this approach.

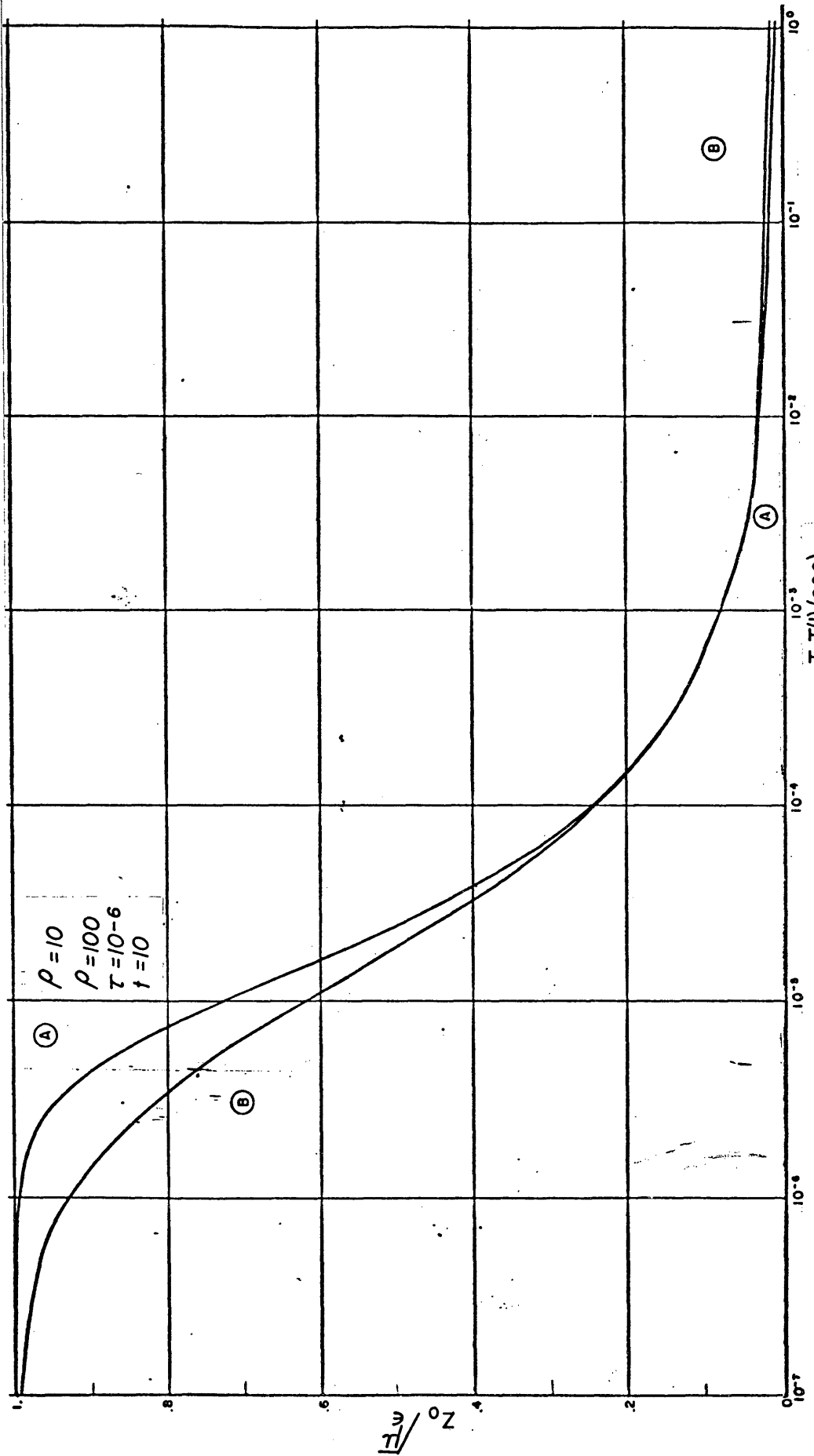


Figure 4: Two-layer case, comparison of harmonic vs. nonharmonic solution

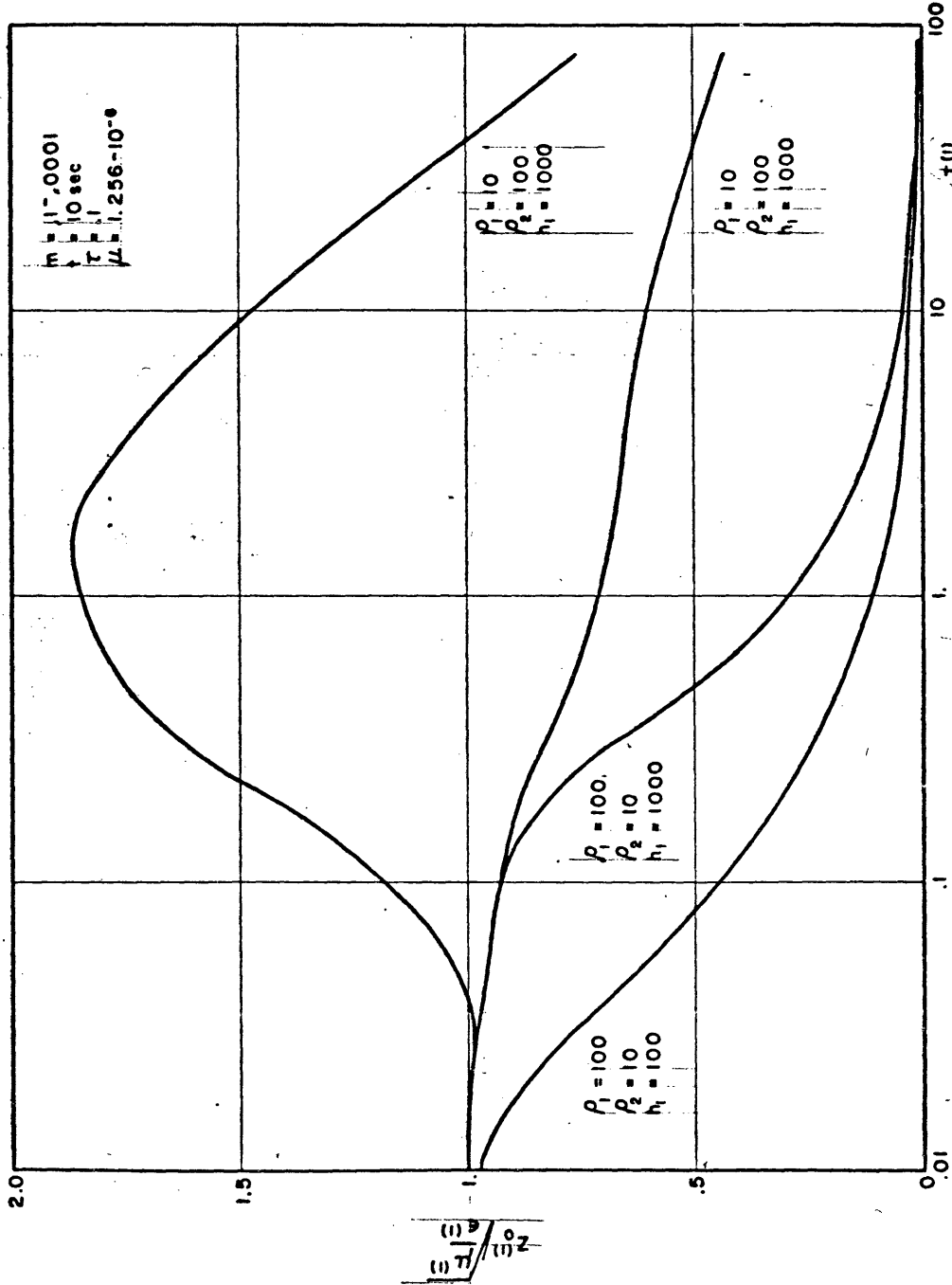


Figure 5: Two-layer case, nonharmonic solution.

F-1879

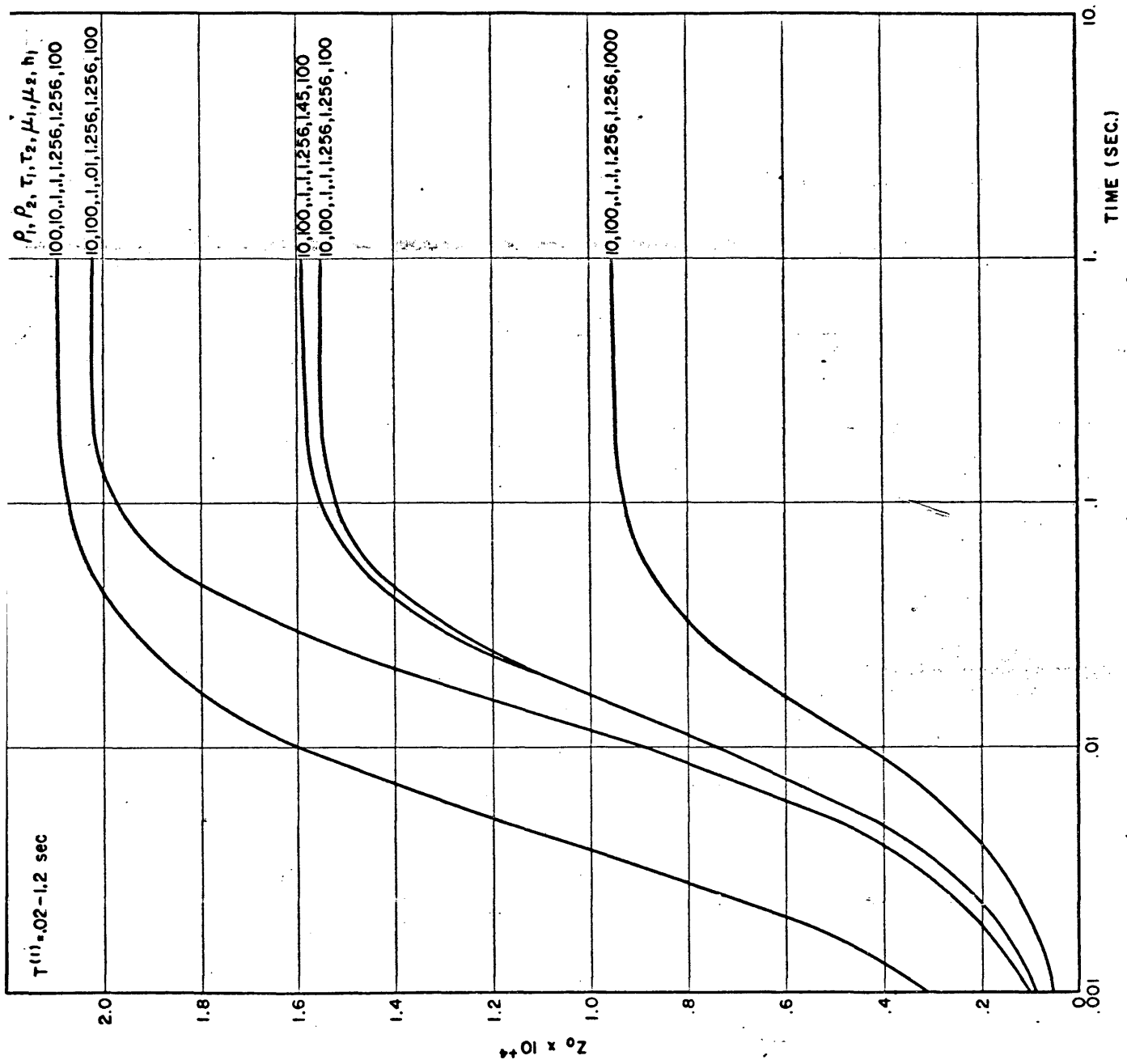


Figure 6: Two-layer case, impedance vs. time

ARTHUR LAKES LIBRARY
COLORADO SCHOOL of MINES
GOLDEN, COLORADO 80401

T-1879

Since we are primarily interested in the change of the impedance vs. time, we now compute;

$$\frac{\partial Z}{\partial t}$$

For the impedance at the surface we have

$$Z_o^{(1)} = E_o^{(1)} / H_o^{(1)}$$

Simplifying the above notation, let

$$Z_o^{(1)} ; E_o^{(1)} = E ; H_o^{(1)} = H$$

or
$$Z = \frac{E}{H}$$

$$\frac{\partial Z}{\partial t} = \frac{1}{H} \frac{\partial E}{\partial t} - \frac{E}{H^2} \frac{\partial H}{\partial t}$$

using $\frac{\partial H}{\partial t} = \frac{1}{\mu} \frac{\partial B}{\partial t}$ we get

$$\frac{\partial Z}{\partial t} = \frac{1}{H} \frac{\partial E}{\partial t} - \frac{E}{H^2} \frac{1}{\mu} \frac{\partial B}{\partial t}$$

$$\frac{\partial Z}{\partial t} = \frac{Z}{E} \left(\frac{\partial E}{\partial t} - \frac{Z}{\mu} \frac{\partial B}{\partial t} \right)$$

T-1879

Or finally

$$\frac{\partial Z}{\partial t} = \frac{E}{B} \left(\frac{1}{E} \frac{\partial E}{\partial t} - \frac{1}{B} \frac{\partial B}{\partial t} \right) \quad (55)$$

Also

$$\begin{aligned} \frac{\partial}{\partial t} \int_0^{\infty} Z(t, m) \, dm &= \frac{\partial}{\partial t} \int_0^{m_{Z_{ss}}} Z(t, m) \, dm \\ &+ \frac{\partial}{\partial t} \int_{m_{Z_{ss}}}^{\infty} Z_{ss}(t, m) \, dm \end{aligned}$$

where $m_{Z_{ss}}$ is the eigenvalue where the impedance Z reached the steady-state value Z_{ss} . However Z_{ss} is constant, hence

$$Z_t(t) = \frac{\partial}{\partial t} \int_0^{\infty} Z(t, m) \, dm$$

$$= \frac{\partial}{\partial t} \int_0^{m_{Z_{ss}}} Z(t, m) \, dm \quad (56)$$

The time derivative of the impedance was programmed for the proper range of eigenvalues, i.e. that eigenvalue where the impedance attains a constant value. The results were plotted as a ratio of $Z_{t0}/Z_{t0,\infty}$; where Z_{t0} represents the time derivative of the impedance at the surface of a multi-layered earth (i.e. several layers above an infinite half-space), and where $Z_{t0,\infty}$ is the time derivative at the surface of an infinite half-space possessing the same physical parameters as the first layer of the multi-layered earth. Figures 7 and 8 show graphs of model curves. In Figure 7 only the resistivity of the second layer was changed. In Figure 8 the parameter τ was changed. Figure 9 shows an example of two layers above a half-space. Some general features emerge from the model curves. The beginning portion of the curves represents information on the surface layer, the last portion of the curve gives information on the underlying half-space. The last portion of the curve approaches a limiting value that is approximately equal to the ratio of the resistivity of the half-space to that of the first layer. For the early time portion of the model curve the ratio of a multi-layer impedance time derivative to that of the impedance time derivative of an infinite half-space approaches 1.0. In order to utilize this information field data need to be recorded using time

intervals of one to several milliseconds. This is not a severe requirement when considering that seismic data are recorded on this time scale. Curve matching procedures then require that an impedance derivative needs to be found which, when divided into the field data impedance derivative, give the ratio 1.0 for the beginning portion of the curve. After accomplishing this step by a simple calculation the value of the resistivity of the infinite halfspace (resistive or conductive basement) can be obtained by multiplying the late time ratio in the flat portion of the curve by the resistivity of the first layer. Intermediate layers require the adjustment of layer thicknesses, resistivities, and the parameter τ .

A change in the parameter τ is seen to have negligible effects on these relationships. The parameter τ primarily produces time shifts in the model curves. It should be stressed that the slowly rising portion of the impedance as observed on the field data is best explained by using values for τ in the same range of magnitudes as those published for induced polarization data. This should not be surprising considering the fact that square wave current pulses constitute the source in induced polarization field techniques.

The development of the time domain approach as presented here shows an approach to obtain magneto-telluric data by way of a controlled source. Model curves can be constructed similarly to those in use with the frequency domain approach. In order to reduce the number of variables in the construction of model curves it might be advantageous to utilize the variables $\tau (= \rho \epsilon)$ and $c (= 1/\sqrt{\mu \epsilon})$ that were introduced in the theoretical development. Since it was not intended to neglect the induced polarization effect, ϵ represents the apparent dielectric constant. This effect is attributed to electrode reactions between the rock and the pore fluid. In the time domain induced polarization method a square current pulse is transmitted into the ground. A transient voltage decay and build-up is associated with each current pulse. Assuming that the time integral of the voltage transient represents storage capacity of the earth material for electrical charge one arrives at the expression $\tau = \rho \epsilon$ where ϵ is now defined as the apparent dielectric constant of the material. The term apparent dielectric constant has been used in the literature to differentiate these low frequency rock properties associated with molecular phenomena from displacement currents associated with electron movement.

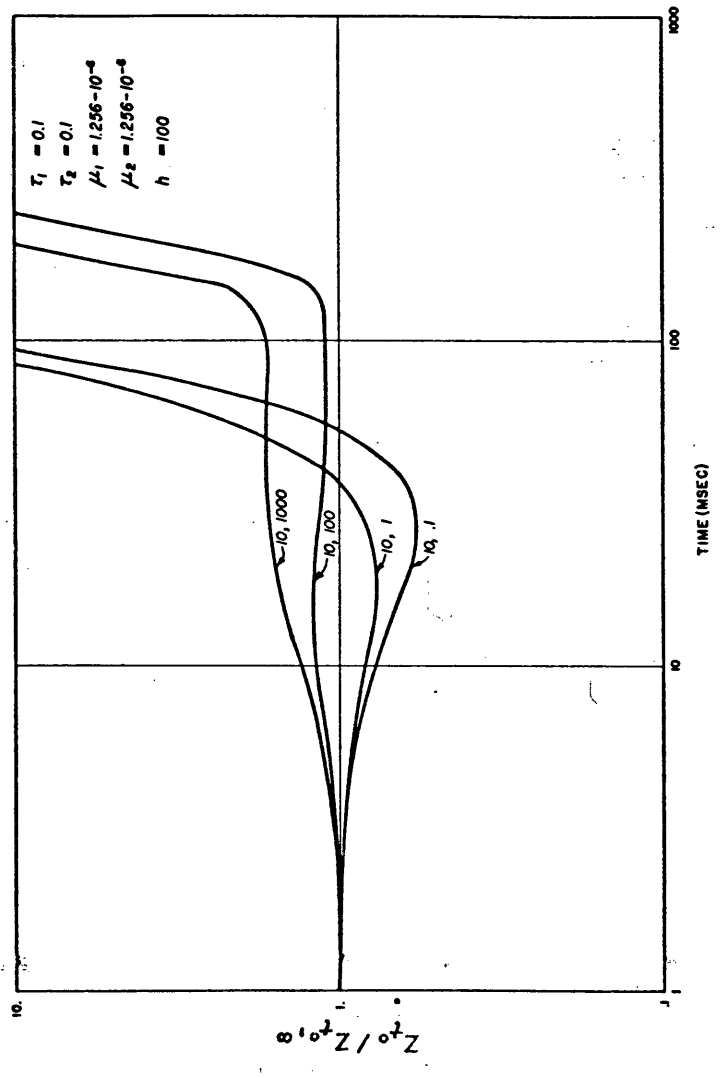


Figure 7: Model curves, time derivative of impedance vs. time, showing the effect of varying second layer resistivity

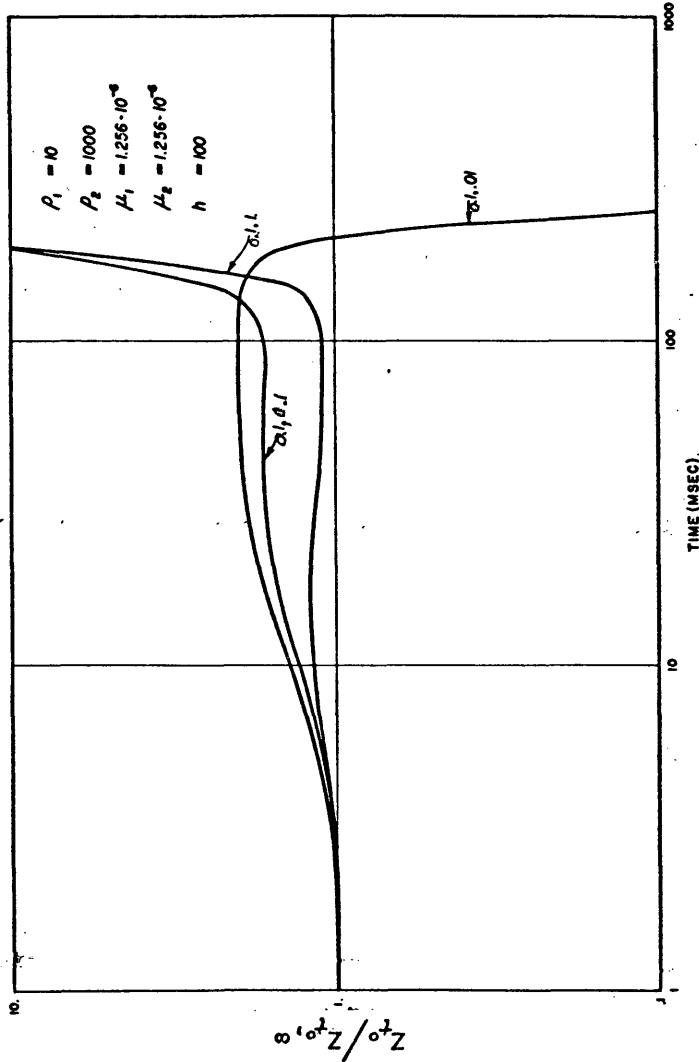


Figure 8: Model curves, time derivative of impedance vs. time, showing the effect of varying the parameter $\tau = \rho \epsilon$

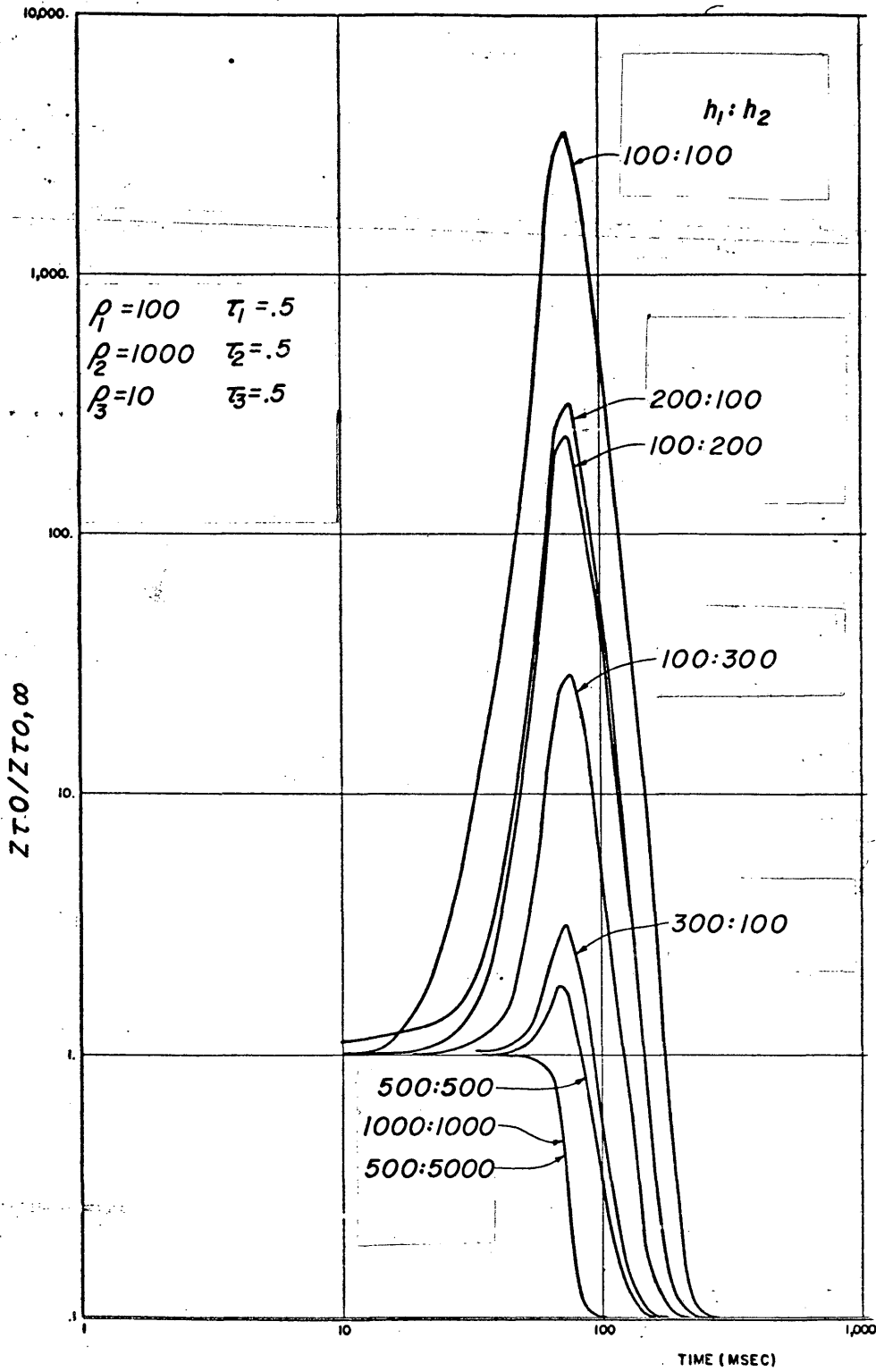


Figure 9: Model curves, three-layer case, showing the effect of varying the layer thickness

Evaluation of the Field Data

The field data that are analysed in this work were not specifically gathered for the theoretical approach presented earlier. However they represent the best data currently available to the author.

These data were collected during the "Long-Line Experiment". This experiment consisted of transmitting current steps along a grounded powerline and measuring the generated electro-magnetic fields some distance away. The powerline utilized for this experiment was the Pacific Northwest-Southwest High-Voltage Direct-Current (HVDC) Transmission Line from the Columbia River to Los Angeles. This line is more than 1,000 km long. These data were collected by the Geophysics Department of the Colorado School of Mines (CSM) during the summer of 1971. The data and the details of the data collection and evaluation were supplied to the author by the Geophysics Department of CSM. A field location map from an unpublished report has been included on p. 49.

The experiment consisted of transmitting direct current pulses of five minutes duration followed by five minutes of off periods. The rise time of the transmission line was within a few milliseconds and hence considered negligible. The magnitude of the current steps was 290

amperes. The resulting electro-magnetic fields were recorded at distances of 20 to 80 kilometers from the HVDC powerline. For distances beyond 60 kilometers noise interference on some of these field data were formidable. The closest surveys were at about 20 kilometers from the line. Furthermore both the electric and magnetic fields were not recorded at every station.

The field procedure for measuring the two orthogonal E- field components consisted of laying out two lengths of wire (250 feet long) grounded through electrodes. The magnetic field data were obtained by means of a horizontal induction loop. This loop consisted of a multi-conductor wire (26 turns) laid out in a square (side length 250 feet) on the ground. The recorded signal was filtered both with a 20-hertz high-cut and a 60-hertz powerline interference filter. Time fiducials were recorded at 0.9- second intervals. The loop served as an induction coil measuring the vertical component of the time rate of change of the magnetic field. This type of field procedure is not used for the field data acquisition in magneto-tellurics, however, for the conversion of vertical component magnetic field data to horizontal component magnetic field data suitable theory was available (Keller, verbal comm.). As explained earlier the theory converts the vertical component of the

ARTHUR LAKES LIBRARY
COLORADO SCHOOL of MINES
GOLDEN, COLORADO 80401

magnetic field recorded with a loop at the receiver station some distance away from a long line wire source to the horizontal component of the magnetic field at right angles to the total electric field recorded at the receiver station. The result of this theoretical conversion is then equivalent to what would be measured by a pair of horizontal induction coils placed onto the ground at right angles to each other. Obviously a direct measurement of this field component with induction coils is superior to that of a theoretical conversion.

The events marked on Figures 10-12, 14-16, 18-20 were digitized by hand using graph paper and a light table. The amplitudes given are those read from the zero reference line marked on the figures. This reference line was established by fitting a reasonable smooth line through the noise preceding the event. Zero reference time was not recorded; hence zero time for each event was picked where the smoothed event departs from the zero reference line. As stated earlier the magnetic field data were obtained by placing an induction loop on the ground. This measures the voltage induced into the coil due to the time rate of change of the vertical component of the magnetic field.

We have

$$\text{e.m.f.} = NA\mu \frac{\partial H}{\partial t}$$

where N = number of turns

A = area of coil

$$\mu = 1.256 \cdot 10^{-6}$$

The H_z field was computed by numerical integration on the computer. The following expression was used to relate the vertical component of the magnetic field to the horizontal component of the magnetic field (see Keller and Frischknecht, 1966, p. 310 for assumptions used in its derivation):

$$\frac{H_x^2}{x} = \frac{2I^3}{(2\pi x)^3 H_z} \quad \text{where, } I = \text{line source current}$$

$$x = \text{source-receiver distance}$$

Inaccuracies introduced by this approximation are probably small compared to other inaccuracies introduced by the data reduction process employed. Some difficulties are also encountered with the electric field data. Superimposed upon the electric field data are the d.c. components established by the current signal input from the powerline. These d.c. components appear to be sizable on some events. In addition the E-fields contain telluric noise drift. A correction was applied to the E-fields for the d.c. components by subtracting a constant estimated from the field records. The electric field components were taken to be at a 90 degree angle in the computation of the resultant vector.

T-1879

The final computation of the impedance involves the ratio of the total E-field and the component of the H_x field projected onto an axis at right angles to the resultant E-field (Mining Geoph., p. 138). The next step is the computation of the derivative of the impedance.

The analysis of the field data was included to demonstrate the interpretative methodology employed in evaluating time domain data in connection with the theoretical approach developed earlier. From all the data obtained in the "Long Line Experiment" the best three examples were chosen, i.e. those with a minimum amount of noise interference. The computed impedances of these three surveys 4W, 6W, and 9W were plotted on Figures 13, 17, 21. The field data for survey 4W are on Figures 10, 11, 12, those for survey 6W are on Figures 14, 15, 16, and those for survey 9W are on Figures 18, 19, 20. A map of the location of these surveys has been included on page 49. Information on electrical parameters and layer thicknesses is contained in the ascending portion of the slope of the impedance. It becomes immediately apparent that it would have been preferable to record the field data at much faster paper speeds. Information necessary to obtain surface layer information can be seen on the model curves to be contained in about the first 20 milliseconds of the rising portion of the slope. Only the best event was picked on each field record.

Hence it was necessary to obtain first layer resistivity information by other means. First layer resistivities for the survey areas are approximately 10 ohm-meters (Keller, verbal comm.). This value was chosen for the further reduction of the data; i.e. the derivative of the impedance was divided by the derivative of the impedance of an infinite half space of resistivity of 10 ohm-meters. The resulting data were plotted on Figure 22. This is the final form in which the field data can then be curve-matched. Only 9W is seen to fall into a range lending itself to the next step of computer curve matching. For this next step a three layer representation appears appropriate for survey 9W.

The rising portion of the impedance is analysed, i.e. the positive portion of the time derivative of the impedance is divided by that of an infinite half-space, and the result is matched to a theoretically computed curve. The actual resistivity distribution with depth at that particular location in the Basin and Range province is of secondary interest only. A possible interpretation (see Figure 23) would be; 235 meters of surface material of resistivity 10 ohm-meters, 500 meters of sediments most likely rich in clay with saline groundwater with a resistivity of .5 ohm-meters, and a more highly resistive layer of 100 ohm-meters at a depth of 735 meters.

ARTHUR LAKES LIBRARY
COLORADO SCHOOL of MINES
GOLDEN, COLORADO 80401

The field data for survey 9W has been plotted together with a theoretical curve on Figure 23. Recalling the field data quality and simplifying assumptions employed in the data reduction it appears to be a reasonable close fit throughout the major portion of the field data. The parameters used in the computation of the matched theoretical curve are given on Figure 23 and in Appendix B.

The example of an actual curve match was included to demonstrate the data reduction technique. As was noted earlier the "Long-Line Experiment" was conducted prior to the existence of the theory presented here, hence at only some of the 73 stations sufficient information was recorded to be useable. The locations of the field surveys are shown on Figure 24. To serve for the purpose of demonstrating the theory both the electric and magnetic fields had to be recorded.

As a result of inexperience with the technique it took an undue amount of time and expense in matching just a single curve. However, the interpretation technique can ultimately be made much cheaper than the conventional curve-matching computer techniques commonly used in resistivity work. This requires a set of model curves to arrive at a first fit. The final match could be accomplished by an iterative computer curve matching program adjusting thickness, resistivity, and

the parameter incrementally. Initially the program utilized 5,000 to 10,000 intervals per integration; however, a reduction to 500 intervals gives comparable results. A reduction in the number of time intervals used to define a curve would result in further time savings.

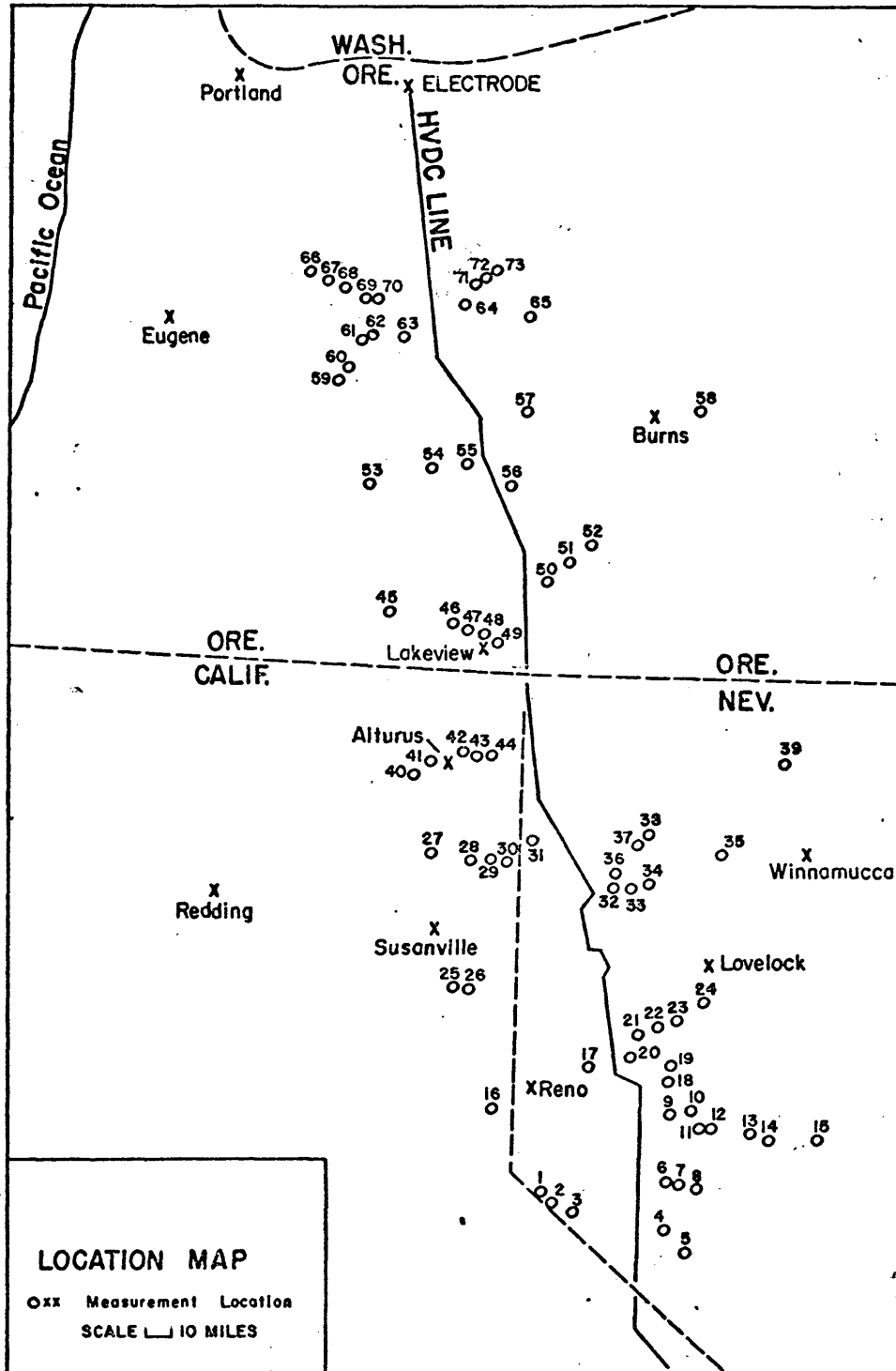


Figure 9a: Survey location map

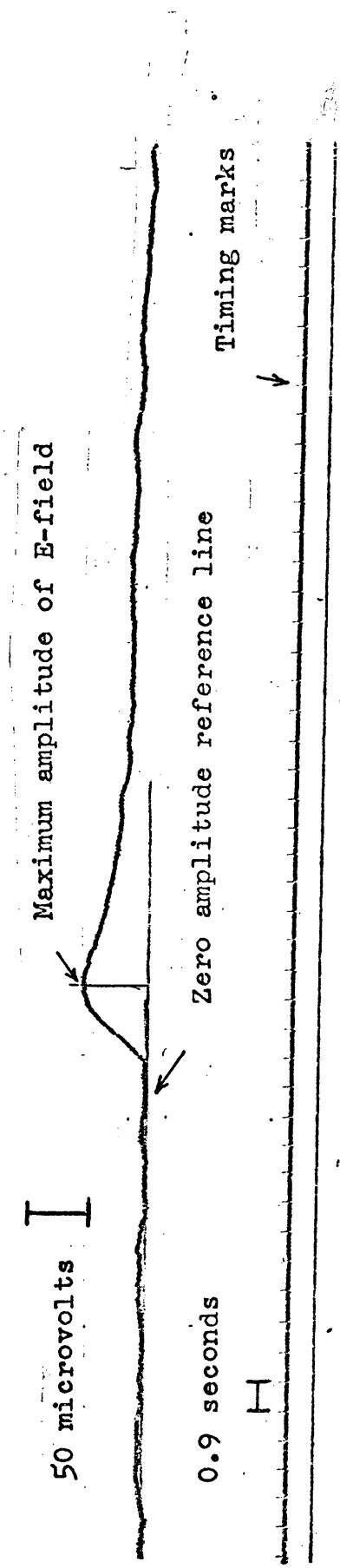


Figure 10: Station 4W, E-field, parallel component

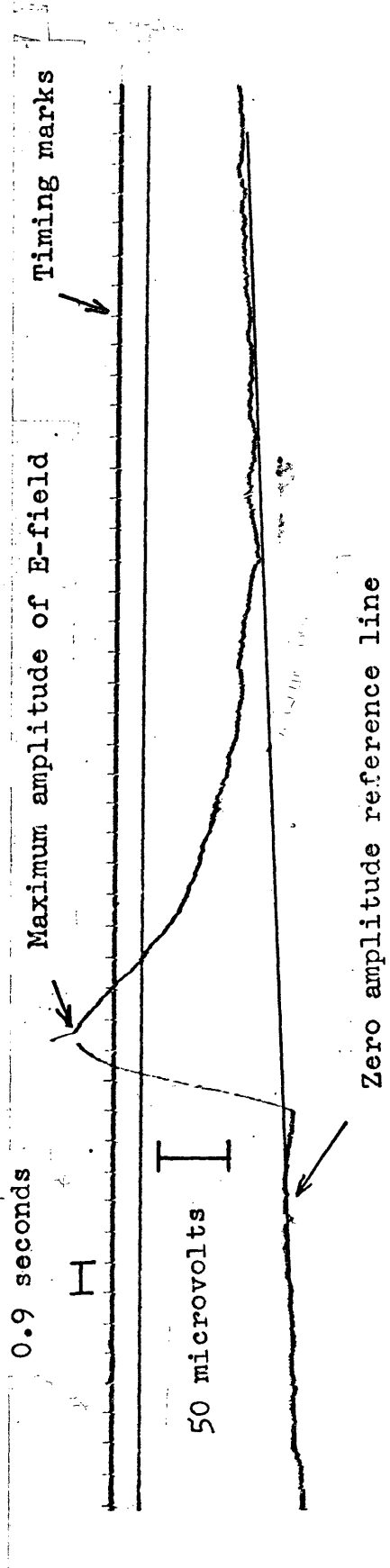


Figure 11: Station 4W, E-field, perpendicular component

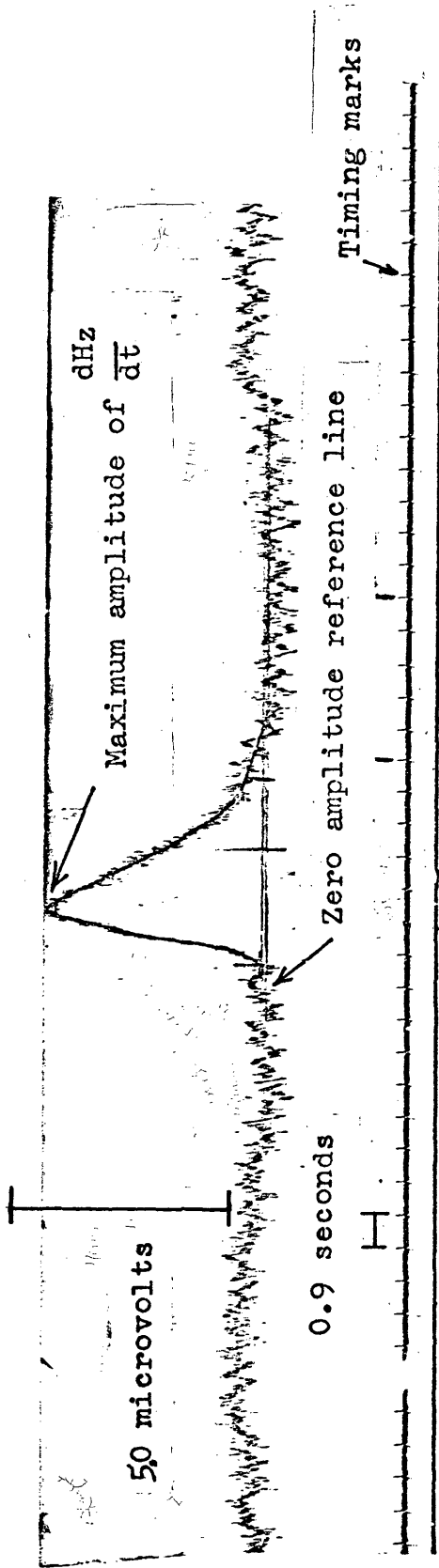


Figure 12: Station 4W, loop data

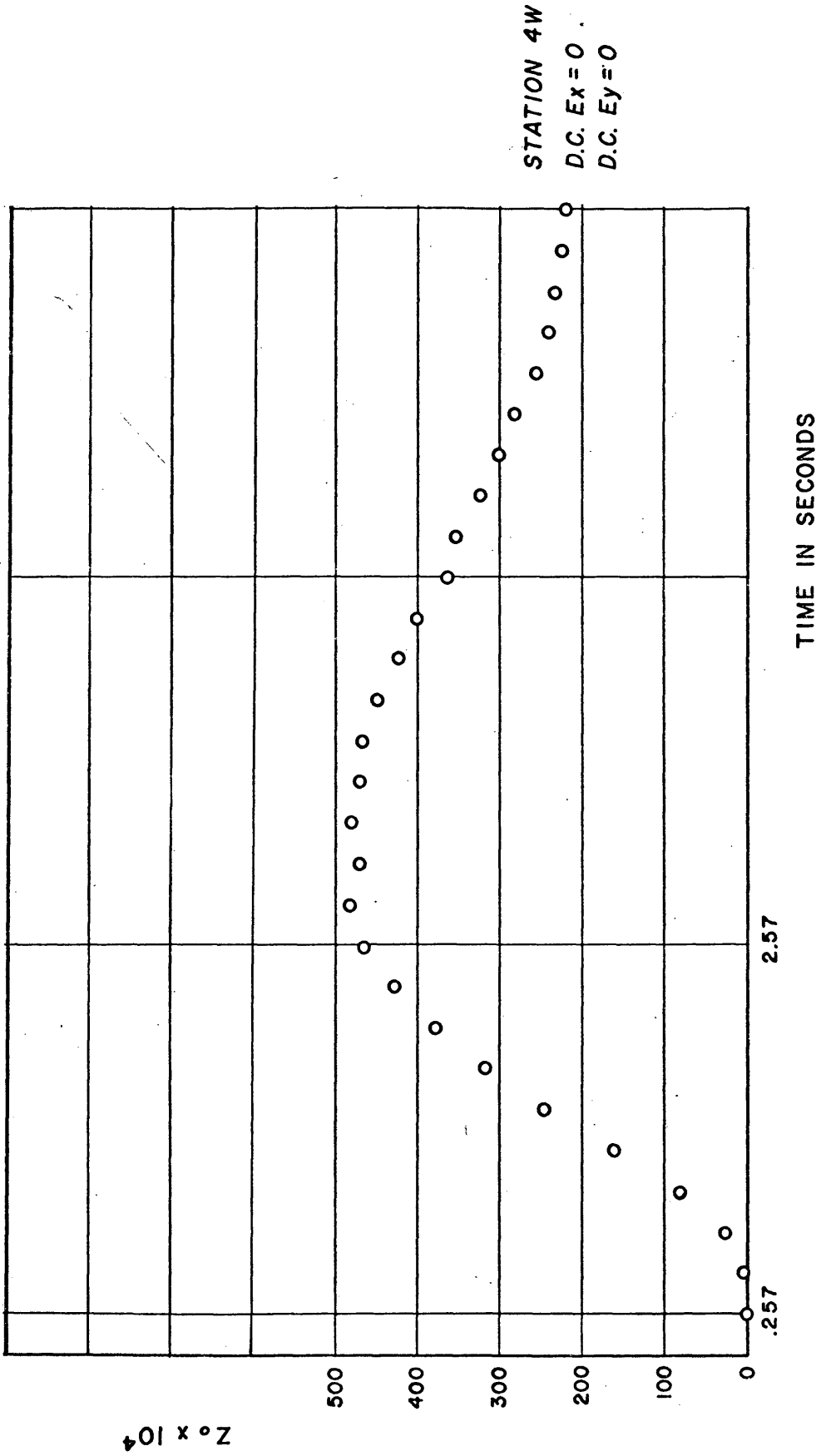


Figure 13: Station 4W, impedance vs. time

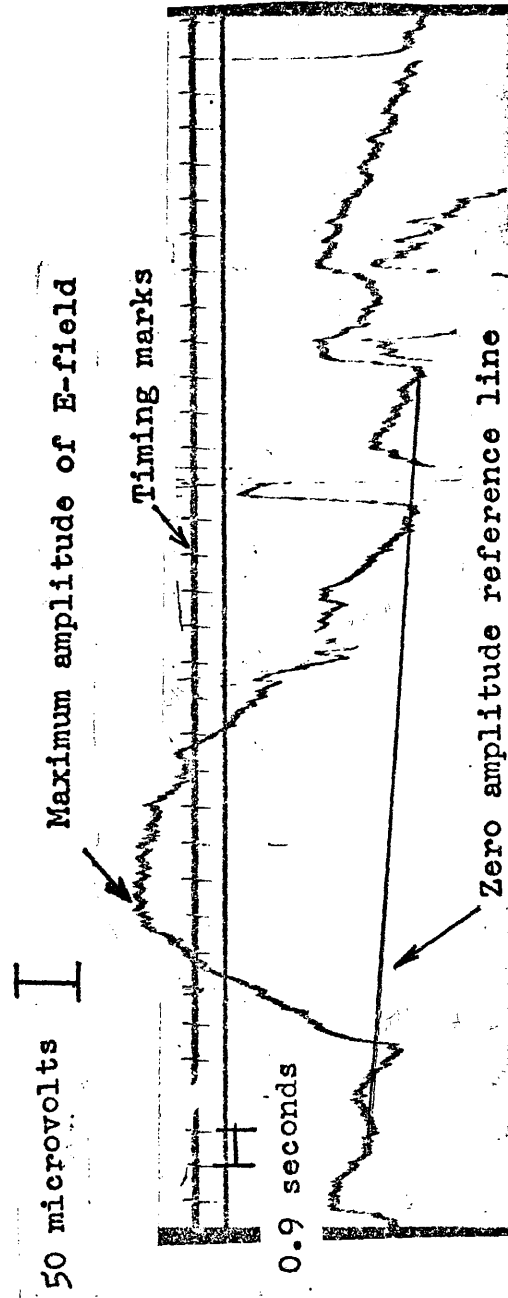


Figure 14: Station 6W, E-field, parallel component

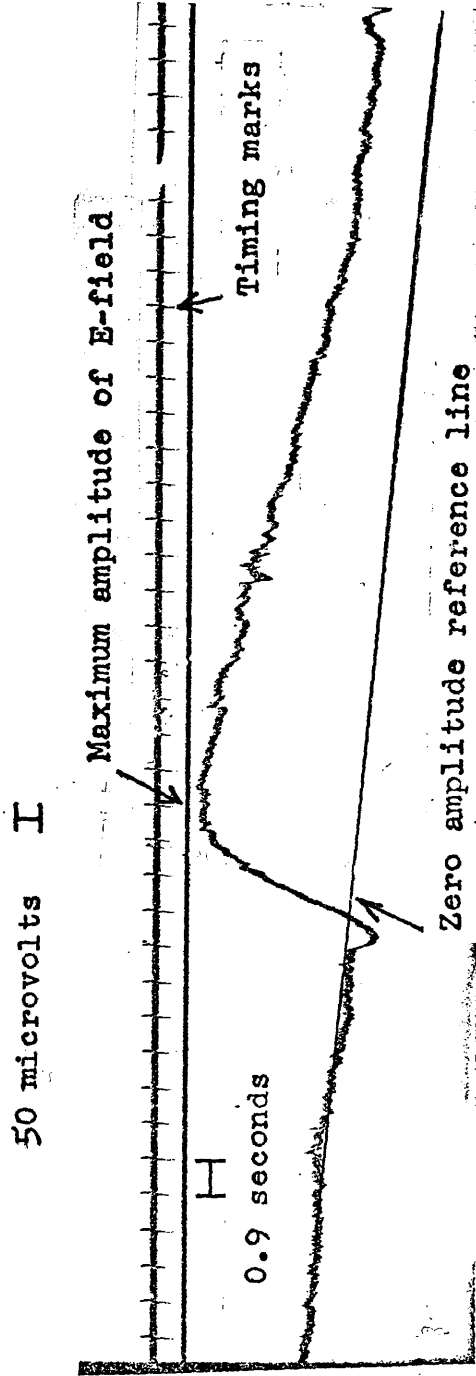


Figure 15: Station 6W, E-field, perpendicular component

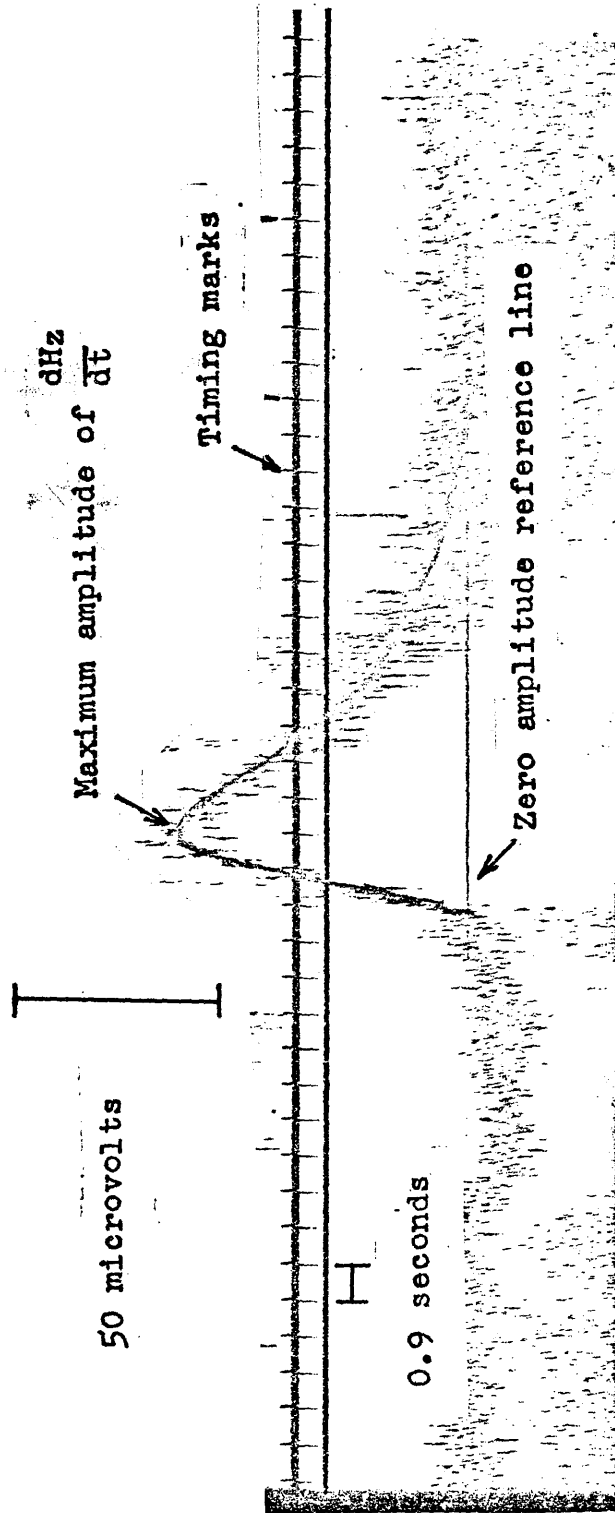


Figure 16: Station 6W, loop data

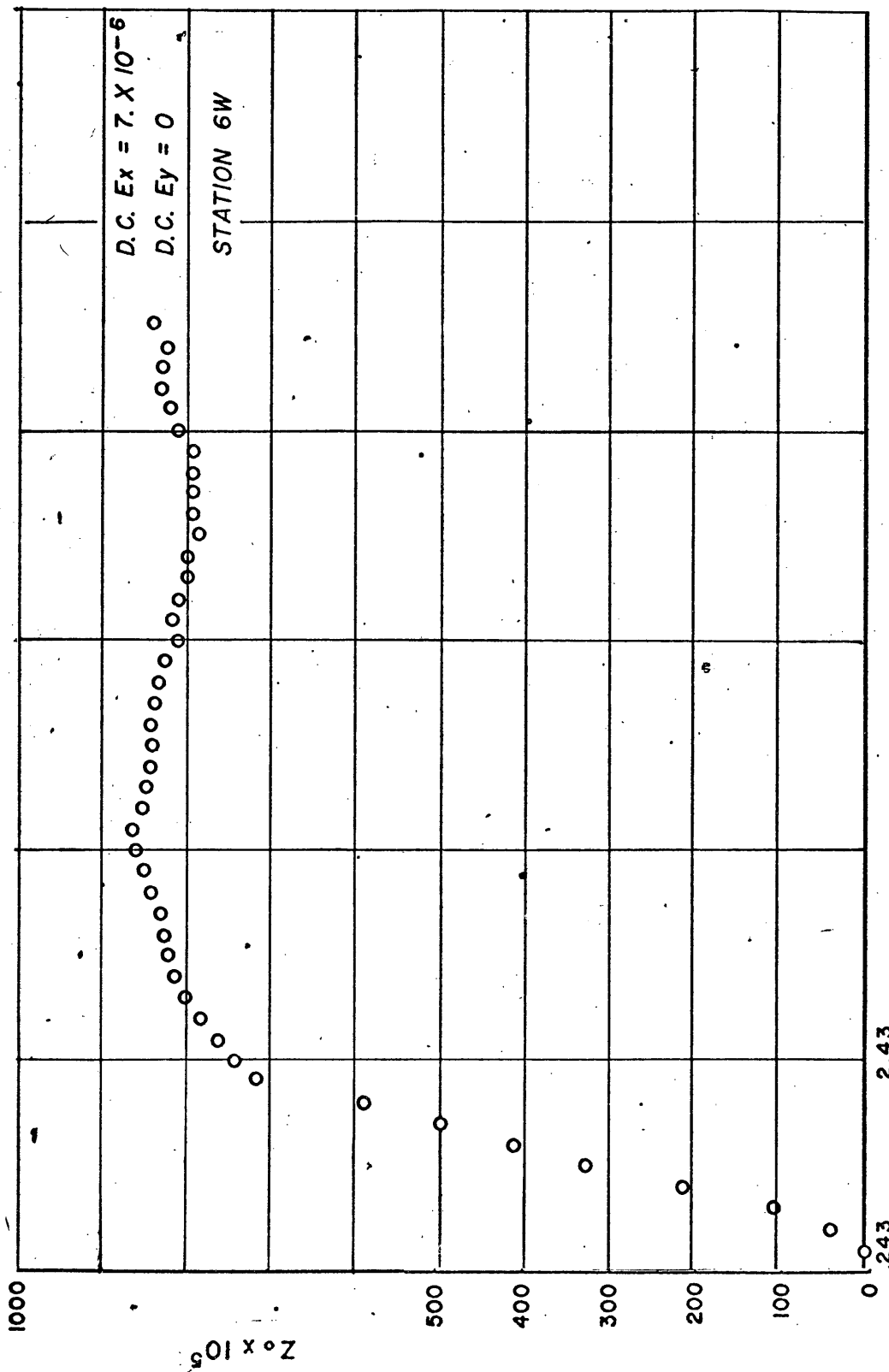


Figure 17: Station 6W, impedance vs. time

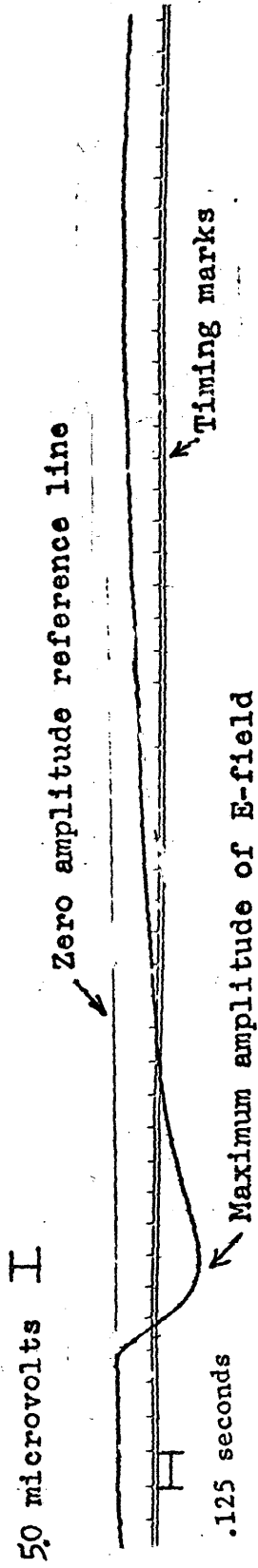


Figure 18: Station 9W, E-field, parallel component

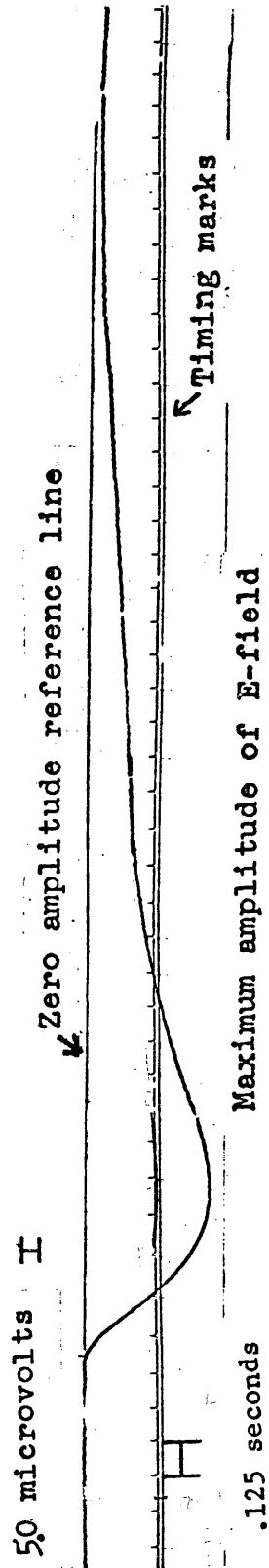


Figure 19: Station 9W, E-field, perpendicular component

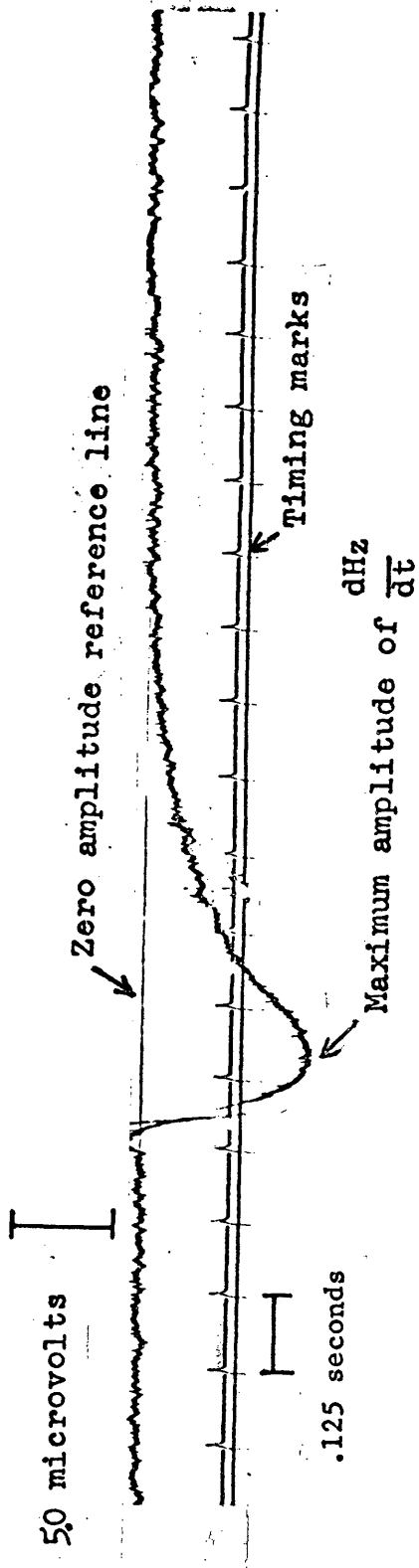


Figure 20: Station 9W, loop data

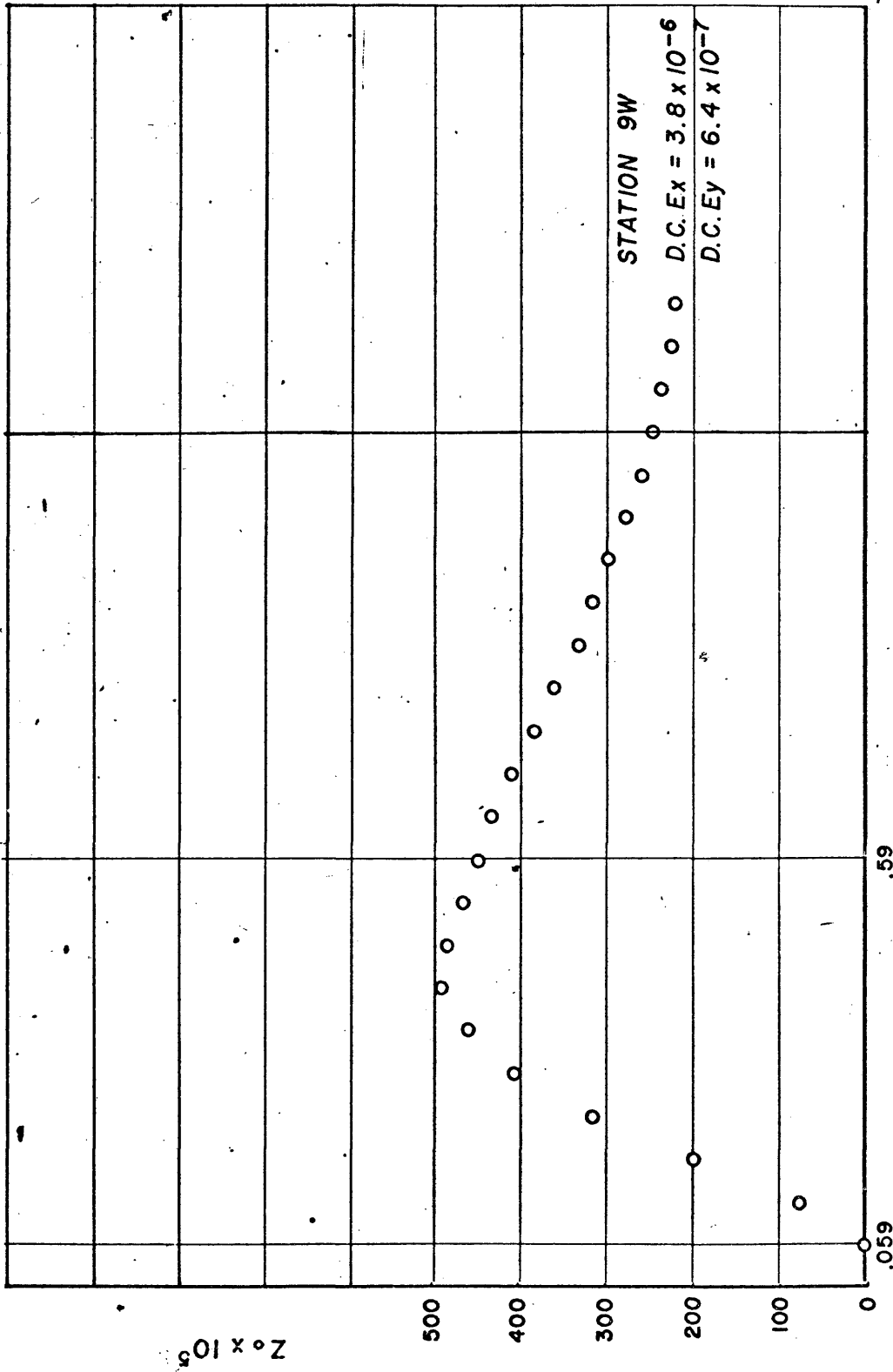


Figure 21: Station 9W, impedance vs. time

T-1879

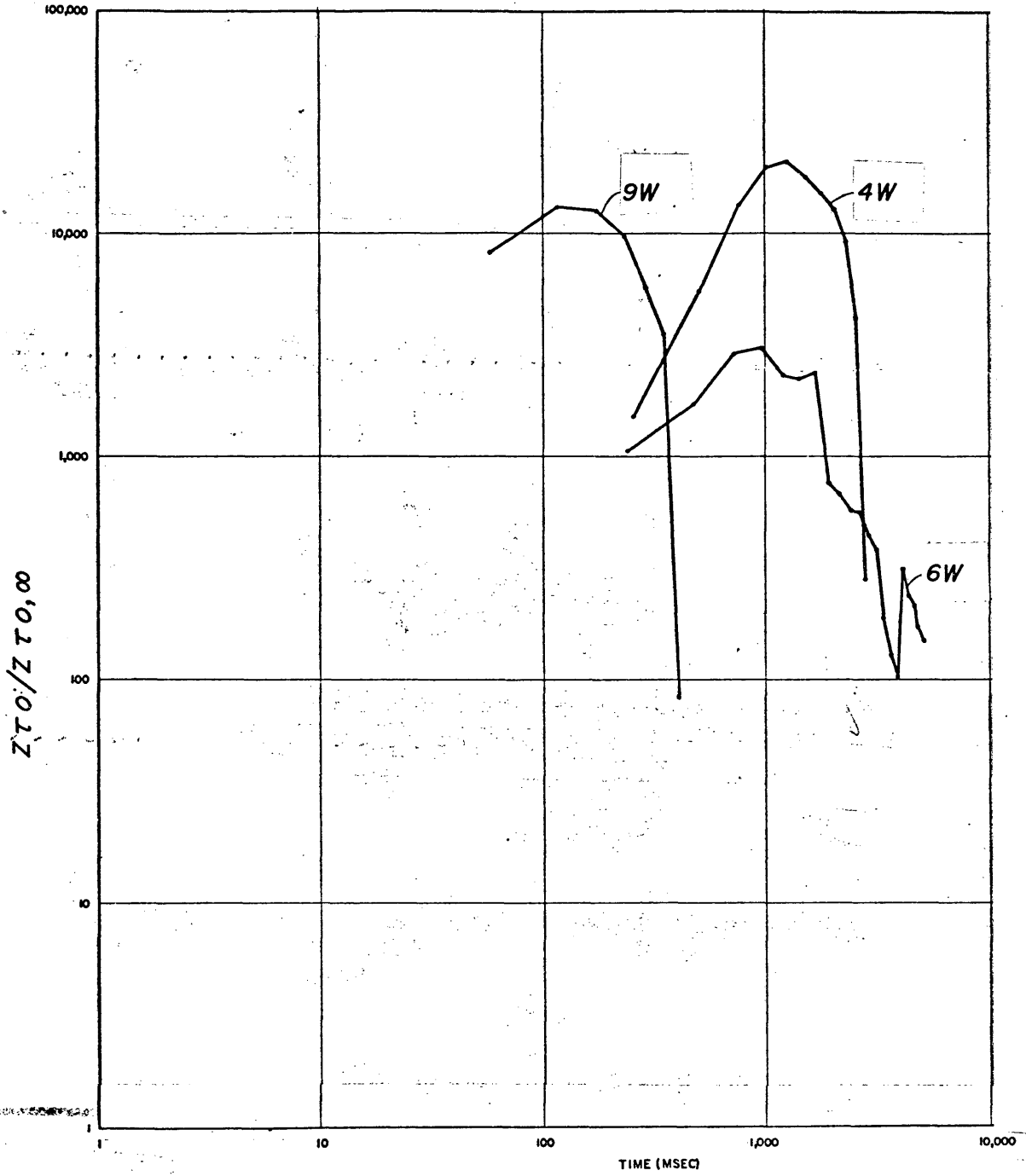


Figure 22: Ratio of field data and half space

T-1879

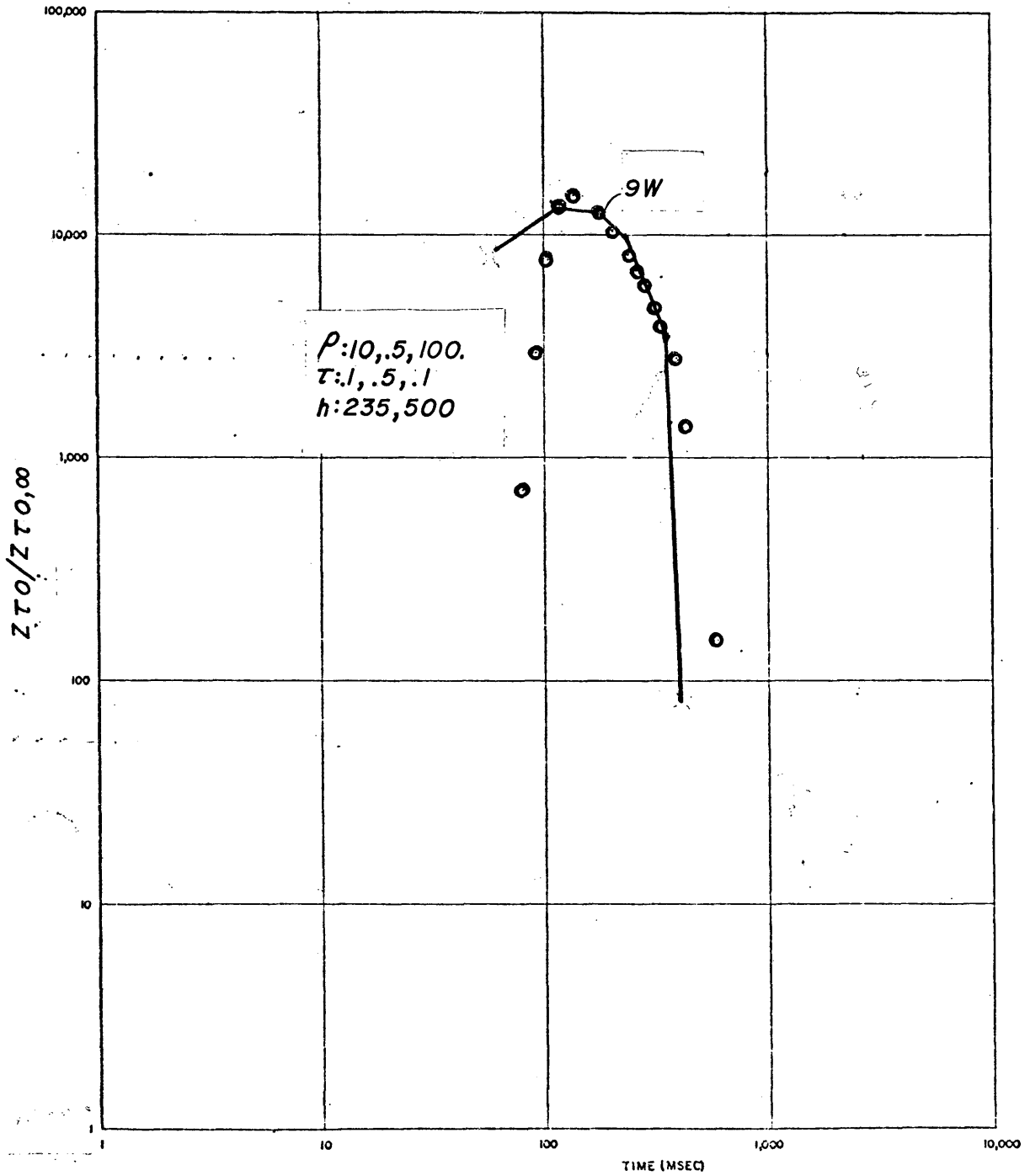


Figure 23: Station 9W, Example of computer curve matching

CONCLUSIONS

The results of this thesis are briefly listed below:

1. A time domain theory was developed for the magnetotelluric depth sounding technique using a current step for a controlled source.
2. A computer program was developed for the generation of model curves.
3. The time domain theory was compared to the frequency domain approach in terms of theoretical implications, data analysis, and field technology.
4. The effects of the magnetic permeability and the apparent dielectric constant, both neglected heretofore, were analyzed in addition to resistivity and layer thicknesses.
5. An example of the field data from the HVDC powerline was analyzed to demonstrate the data reduction and interpretation technique developed here.
6. A field technique suitable for routine electrical exploration depth sounding was proposed.

In order to compare this novel time domain electrical sounding method with other established technology, the controlled source MT survey could be conducted in conjunction with a resistivity survey to obtain resistivities independently.

The controlled source method is capable of overcoming problems normally encountered in recording weak natural fields often containing insufficient frequency information. The analysis of field data in the frequency domain suffers from amplitude distortions that are a result of random signal content and signal truncation errors. These problems are eliminated with the time domain approach.

The analysis of the field data in the time domain illustrates some of the weaknesses of the time domain approach. Noise interference can be severe at large distances. Filtering should be applied with caution. Signal stacking, however, can overcome most background noise problems. Field data acquisition should be modified to employ horizontal induction coils.

It appears that experience with the time domain method should be gained in areas well explored with other electrical methodology. The time domain controlled magnetotelluric method as developed here is seen to have enough advantages where it can with proper changes in field procedure and instrumentation replace most conventional methods and become a useful exploration tool for electrical exploration.

T-1879

APPENDIX A

Program Description - ZRATIO

Programs ZRATIO compute the ratio of the derivative of the impedance of a multi-layered case to that of an infinite half space. Program ZRATIO1 incorporates equation (32), program ZRATIO2 uses equation (54). The input and output are identical in format. All input units have to be in the MKS system. Representative magnitudes for the parameter $\tau = \rho \epsilon$ have been obtained from published values (see Keller and Frischknecht, 1966, p. 463). As a result of numerical experimentation on the computer for a variety of cases the range of eigenvalues used in the integration (see equation 56) has been fixed in the program. The number of intervals used in this integration has also been selected in the program.

The program flow is as follows:

At a given time "t" the impedance is computed by evaluating the integral (equation (1)) over an adequate range (XMIN, XMAX) of the eigenvalue. Then the derivative of the impedance is done for both the multilayered case and also the infinite half space. The physical parameters picked for the infinite half space are identical to those for layer 1 in the multilayered case. By forming the ratio of the two time derivatives of the impedances it can be seen

T-1879

that for small enough times this ratio approaches one.

This results in a model curve display that is more easily interpreted.

Input Parameters:

MAXTIME total number of points on time axis for which program computes model curves. Format, I2, maximum = 30 points (subject to restriction see TIMAX)

NUMLAY number of horizontal layers, including half space. Format I1, maximum = 5

TIMIN starting time for which curve is computed in seconds, minimum (0.001 second)

TIMAX endtime for which model curve is computed (subject to restriction - see MAXTIME)

The time increments are computed as follows:

$$T_{in} = t_i \times 1.1$$

U(K) permeabilities for K layers

RHO(K) resistivities for K layers

EPSRHO(K) parameter for K layers

Z(K) thicknesses for horizontal layers; total number = NUMLAY-1

The input parameters are entered into the program as follows:

T-1879

Line

1	MAXTIME, NUMLAY
2	TIMIN, TIMAX
3	U(K)
4	RHO(K)
5	EPSRHO(K)
6	Z(K)

Program Description - Data

Program DATA was written to aid in the evaluation of the field data obtained by the "Long Line Experiment." The program has been included in order to help expedite the processing of field data collected with an equally applicable field technique.

The program operates as follows: Field data that were hand-digitized on graph paper at equal time intervals are input into the computer. The input consists of E-field data perpendicular to the source (E_x), parallel to the source (E_y), the horizontal loop data, i.e., the time rate of change of the magnetic field (marked H_z on the field data). Furthermore, the proper time interval and amplitude interval per increment of graph paper must be listed consistent with the MKS system. Corrections for dc-components, if applicable, must be entered for the E-fields. Other input data required are the number of samples, number of turns and size of loop to obtain H-field information,

T-1879

distance of survey from source, and source current strength. In addition, physical parameters must be assumed for an equivalent semi-infinite half space. The program first converts the digitized values into true amplitudes and times. It then computes the magnitude and direction of the resultant E-field. The horizontal loop data are converted to the vertical component of the H-field by numerical integration. From this result the equivalent horizontal H-field is computed and projected onto an axis at right angles to the resultant E-field. The next steps are the computation of the impedance and its time derivative. Then the ratio is formed from the field data time derivative and that of the assumed infinite half space.

Input Parameters:

J	line number identification
TURNS	number of turns in horizontal loop
AREA	loop area in m ²
R	distance of survey from source in meters
AMP	source current in amperes
NT	number of digitized samples
VEY	amplitude of perpendicular E-field in volts per graph paper division
VEY	amplitude of parallel E-field in volts per graph paper division

T-1879

VDBDT amplitude of horizontal loop data in volts
 per graph paper division

TI length of time interval on graph paper in
 seconds

DCX DC - component of E_x field

DCY DC - component of E_y field

DEX(I) digitized E_x field data

DEY(I) digitized E_y field data

DDBDT(I) digitized horizontal loop data

ZU(K) permeability of half space

RHO(K) resistivity of half space

EPSRHO(K) parameter of half space

THICK(K) thickness - enter zero

The input parameters are entered into the program as follows:

Line

1 J

2 TERMS, Area, R, AMP, NT

3 VEX, VEY, VDBDT, TI, DCX, DCY

4 DEX(I)

5 DEY(I)

6 DDBDT(I)

7 U(K)

8 RHO(K)

9 EPSRHO(K)

10 THICK(K)

T-1879

```

PROGRAM ZRATIO1 (INPUT, OUTPUT, TAPE1=INPUT, TAPE2)
DIMENSION T (50), U (5), RHO (5), EPSRHO (5), Z (5)
DIMENSION B (5), XINTG (50)
READ (1, *) MAXTIME, NUMLAY
XMMAX=3.

```

```

XMMIN=1.E-09

```

```

C XMAX, XMMIN ARE THE MAXIMUM AND MINIMUM VALUES OVER WHICH THE
C INTEGRATION OF THE EIGENVALUES IS CARRIED OUT

```

```

INT=500

```

```

C INT REPRESENTS THE TOTAL NUMBER OF INTERVALS USED IN THE
C INTEGRATION OF THE EIGENVALUES

```

```

LXMIN=1

```

```

INTM=1

```

```

NULAY=NUMLAY-1

```

```

READ (1, *) TIMIN, TIMAX

```

```

READ (1, *) (U (K), K=1, NUMLAY)

```

```

READ (1, *) (PHO (K), K=1, NUMLAY)

```

```

READ (1, *) (EPSRHO (K), K=1, NUMLAY)

```

```

READ (1, *) (Z (K), K=1, NULAY)

```

```

WRITE (2, *) MAXTIME, NUMLAY

```

```

WRITE (2, *) TIMIN, TIMAX

```

```

WRITE (2, *) (U (K), K=1, NUMLAY)

```

```

WRITE (2, *) (PHO (K), K=1, NUMLAY)

```

```

WRITE (2, *) (EPSRHO (K), K=1, NUMLAY)

```

```

WRITE (2, *) (Z (K), K=1, NULAY)

```

```

NCOUNT=2

```

```

T (1)=TIMIN

```

```

DO 3 J=1, MAXTIME

```

```

3 T (J+1)=T (J)*1.1

```

```

DO 30 M=1, INTM

```

```

C----- COMPUTE EIGENVALUE INTERVAL

```

```

DELXM=(XMMAX-XMMIN)/INT

```

```

4 CONTINUE

```

```

DO 2 J=1, MAXTIME

```

```

CALL GAUSS (XMMIN, Z0, XIGR, Z, NUMLAY, T, U, RHO,

```

```

1 EPSRHO, I, J, B)

```

```

SUMIGR=XIGR*DELXM/2.

```

```

SUMIGI=XIGI*DELXM/2.

```

```

XM=XMMIN+DELXM

```

```

DO 1 I=1, INT

```

```

CALL GAUSS (XM, Z0, XIGR, Z, NUMLAY, T, U, RHO,

```

```

1 EPSRHO, I, J, B)

```

```

XIGR=XIGR*DELXM

```

```

SUMIGR=SUMIGR+XIGR

```

```

1000 FORMAT (2X, 1E10.3)

```

```

XM=XM+DELXM

```

```

IF (XM.GT.XMMAX) GO TO 23

```

```

1 CONTINUE

```

```

23 CONTINUE

```

```

1002 FORMAT (1X, 7HNUMINT=, I4)

```

```

XINTG (J)=SUMIGR

```

T-1879

```

GO TO 13
WRITE(2,1007)T(J),SUMIGR
13 CONTINUE
1007 FORMAT(3X,2HT=,F10.4,3X,2HA=,E10.3)
2 CONTINUE
CALL DELTIME(XINTG,MAXTIME,T,NUMLAY)
NUMLAY=1
NCCOUNT=NCCJNT-1
IF(NCCOUNT.LT.1)GO TO 5
GO TO 4
5 CONTINUE
INT=INT+LXMIN
30 CONTINUE

CALL EXIT
END
SUBROUTINE BJ(T,XM,U,RHO,EPSRHO,I,J,K,B,CMP)
DIMENSION T(200),U(5),RHO(5),EPSRHO(5)
DIMENSION B(5)
XMM=XM*XM
TAU=EPSRHO(K)*2.
C3=1./TAU
TTAU=TAU*TAU
VV=RHO(K)/(U(K)*EPSRHO(K))
V=SQRT(VV)
C1=1./TTAU
WW=XMM*VV+C1
W=SQRT(WW)
1001 FORMAT(2X,1E10.3)
TAUW=TAU*W
C2=1./TAUW
CALL ARTANH(C2,BETA)
WT=T(J)*W
WMT=-WT
A=V*XM
IF(WT.GT.25.)GO TO 40
S1=A*.5*(EXP(WT)-EXP(WMT))
BETAWT=BETA+WT
BETAWMT=-BETAWT
S2=.5*(EXP(BETAWT)+EXP(BETAWMT))
B(K)=-U(K)*S1/S2
GO TO 41
40 BETAM=-BETA
B(K)=-U(K)*A*EXP(BETAM)
41 CONTINUE
OMP=(-C3+W)/6.2831853
RETURN
END
SUBROUTINE IMP(Z,Z0,NUMLAY,T,XM,U,RHO,EPSRHO,I,J,
1B,OMP)

```

T-1879

C SUBROUTINE IMP COMPUTES THE IMPEDANCE AT THE SURFACE OF A
 C MULTILAYERED HALFSPACE AT A GIVEN TIME AND GIVEN EIGENVALUE

DIMENSION T(50),U(5),RHO(5),EPSRHO(5),Z(5)

DIMENSION ZZ(5),B(5)

Z(0)=0.

CALL BJ(T,XM,U,RHO,EPSRHO,I,J,NUMLAY,B,OMP)

ZZ(NUMLAY)=-B(NUMLAY)/XM

IF(NUMLAY.LE.1)GO TO 9

NUMLAY2=NUMLAY+1

NUMLAY1=NUMLAY-1

DO 9 L=1,NUMLAY1

L1=NUMLAY2-L

L2=L1-1

L3=L1-2

H=Z(L3)-Z(L2)

XMH=XM*H

ZZXM=ZZ(L1)*XM

HTAN=TANH(XMH)

CALL BJ(T,XM,U,RHO,EPSRHO,I,J,L2,B,OMP)

BL2=B(L2)

ZZNUM=ZZXM+BL2*HTAN

ZZDEN=ZZXM*HTAN+BL2

FRAC=BL2*ZZNUM/ZZDEN

ZZ(L2)=FRAC/XM

9 CONTINUE

Z0=ZZ(L2)

GO TO 7

8 Z0=ZZ(NUMLAY)

7 CONTINUE

RETURN

END

SUBROUTINE GAUSS(XM,Z0,XIGR,Z,NUMLAY,T,U,RHO,

1 EPSRHO,I,J,B)

C SUBROUTINE GAUSS COMPUTES THE INTEGRAL OVER A RANGE OF
 C EIGENVALUES AT A GIVEN TIME

DIMENSION T(50),U(5),RHO(5),EPSRHO(5),Z(5)

DIMENSION B(5)

DEL1=XM

CALL IMP(Z,Z0,NUMLAY,T,DEL1,U,RHO,EPSRHO,I,J,

1B,OMP)

4010 FORMAT(3X,16HDIVISION BY ZERO)

XIGR=Z0

XIGI=0.

GO TO 33

WRITE(2,4020)DEL1,OMP,T(J),Z0

33 CONTINUE

4020 FORMAT(3X,2HM=,1E10.3,3X,2HF=,1E10.3,3X,2HT=,F10.3,3X,

12HA=,1E10.3)

RETURN

T-1879

```

END
SUBROUTINE ARTANH(X, ATANH)

```

```

C SUBROUTINE ARTANH COMPUTES THE HYPERBOLIC ARCTANGENT

```

```

CP=1.+X
CM=1.-X

```

```

ALOGCP=ALOG(CP)
ALOGCM=ALOG(CM)
ATANH=.5*(ALOGCP-ALOGCM)

```

```

GO TO 32

```

```

31 WRITE(2,5000)

```

```

5000 FORMAT(3X,12HLOG NEGATIVE)

```

```

32 CONTINUE

```

```

RETURN
END

```

```

SUBROUTINE DELTIME(XINTG, MAXTIME, T, NUMLAY)

```

```

C SUBROUTINE DELTIME COMPUTES THE DERIVATIVE OF THE IMPEDANCE

```

```

DIMENSION XINTG(50), T(50)

```

```

DIMENSION ZT(50), ZT1(50)

```

```

DO 4 J=1, MAXTIME

```

```

DELT=T(J+1)-T(J)

```

```

IF(NUMLAY.EQ.1)GO TO 1

```

```

ZT(J)=(XINTG(J+1)-XINTG(J))/DELT

```

```

GO TO 2

```

```

1 ZT1(J)=(XINTG(J+1)-XINTG(J))/DELT

```

```

2 CONTINUE

```

```

2000 FORMAT(3X,3HZT=,E10.3,3X,2HT=,F10.4)

```

```

IF(NUMLAY.GT.1)GO TO 3

```

```

RATIO=ZT(J)/ZT1(J)

```

```

WRITE(2,2001)RATIO,T(J)

```

```

3 CONTINUE

```

```

2001 FORMAT(3X,5HRATIO=,E10.3,3X,2HT=,F10.4)

```

```

4 CONTINUE

```

```

RETURN

```

```

END

```

```

PROGRAM ZRATIO2 (INPUT, OUTPUT, TAPE1=INPUT, TAPE2)
DIMENSION T(50), U(5), RHO(5), EPSRHO(5), Z(5)
DIMENSION B(5), XINTG(50)
READ(1, *) MAXTIME, NUMLAY
XMMAX=5.
XMMIN=1.E-09
C XMAX, XMMIN ARE THE MAXIMUM AND MINIMUM VALUES OVER WHICH THE
C INTEGRATION OF THE EIGENVALUES IS CARRIED OUT
INT=500
C INT REPRESENTS THE TOTAL NUMBER OF INTERVALS USED IN THE
C INTEGRATION OF THE EIGENVALUES
LXMIN=1
INTM=1
NUMLAY=NUMLAY-1
READ(1, *) TIMIN, TIMAX
READ(1, *) (J(K), K=1, NUMLAY)
READ(1, *) (RHO(K), K=1, NUMLAY)
READ(1, *) (EPSRHO(K), K=1, NUMLAY)
READ(1, *) (Z(K), K=1, NUMLAY)
WRITE(2, *) MAXTIME, NUMLAY
WRITE(2, *) TIMIN, TIMAX
WRITE(2, *) (U(K), K=1, NUMLAY)
WRITE(2, *) (RHO(K), K=1, NUMLAY)
WRITE(2, *) (EPSRHO(K), K=1, NUMLAY)
WRITE(2, *) (Z(K), K=1, NUMLAY)
NCGOUNT=2
T(1)=TIMIN
DO 3 J=1, MAXTIME
3 T(J+1)=T(J)*1.1
DO 30 M=1, INTM
C----- COMPUTE EIGENVALUE INTERVAL
DELXM=(XMMAX-XMMIN)/INT
4 CONTINUE
DO 2 J=1, MAXTIME
CALL GAUSS(XMMIN, Z0, XIGR, Z, NUMLAY, T, U, RHO,
1 EPSRHO, I, J, B)
SUMIGR=XIGR*DELXM/2.
SUMIGI=XIGI*DELXM/2.
XM=XMMIN+DELXM
DO 1 I=1, INT
CALL GAUSS(XM, Z0, XIGR, Z, NUMLAY, T, U, RHO,
1 EPSRHO, I, J, B)
XIGR=XIGR*DELXM
SUMIGR=SUMIGR+XIGR
1000 FORMAT(2X, 1E10.3)
XM=XM+DELXM
IF (XM.GT.XMMAX) GO TO 23
1 CONTINUE
23 CONTINUE
1002 FORMAT(1Y, 7HNUMINT=, I4)
XINTG(J)=SUMIGR

```

T-1879

```

GO TO 13
WRITE(2,1007)T(J),SUMIGR
13 CONTINUE
1007 FORMAT(3X,2HT=,F10.4,3X,2HA=,E10.3)
2 CONTINUE
CALL DELTIME(XINTG,MAXTIME,T,NUMLAY)
NUMLAY=1
NCCOUNT=NCCOUNT-1
IF(NCCOUNT.LT.1)GO TO 5
GO TO 4
5 CONTINUE
INT=INT+LXMIN
30 CONTINUE

CALL EXIT
END
SUBROUTINE BJ(T,XM,U,RHO,EPSRHO,I,J,K,B,OMP)
C SUBROUTINE BJ COMPUTES EXPRESSION B(J), I.E. THE TIME
C FUNCTION FOR A GIVEN LAYER AT A GIVEN TIME AND GIVEN EIGENVALUE
DIMENSION T(50),U(5),RHO(5),EPSRHO(5)
DIMENSION B(5)
XMM=XM*XM
TAU=EPSRHO(K)*2.
C3=1./TAU
TTAU=TAU*TAU
VV=PHO(K)/(U(K)*EPSRHO(K))
V=SQRT(VV)
C1=1./TTAU
WW=XMM*VV+C1
W=SQRT(WW)
1001 FORMAT(2X,1E10.3)
TAUW=TAU*W
C2=1./TAUW
WT=T(J)*W
WMT=-WT
A=V*XM
TANHWT=TANH(WT)
S1=2.*TTAU*XMM*VV*TANHWT
S2=2.*TTAU*W+TANHWT
B(K)=-U(K)*S1/S2
GO TO 41
40 BETAM=-BETA
B(K)=-U(K)*A*EXP(BETAM)
41 CONTINUE
OMP=(-C3+W)/6.2831853
RETURN
END
SUBROUTINE IMP(Z,Z0,NUMLAY,T,XM,U,RHO,EPSRHO,I,J,
1B,OMP)
C SUBROUTINE IMP COMPUTES THE IMPEDANCE AT THE SURFACE OF A

```

T-1879

```

C — MULTILAYERED HALFSpace AT A GIVEN TIME AND GIVEN EIGENVALUE
DIMENSION T(50),U(5),RHO(5),EPSRHO(5),Z(5)
DIMENSION ZZ(5),B(5)
Z(0)=0.
CALL BJ(T,XM,U,RHO,EPSRHO,I,J,NUMLAY,B,OMP)
ZZ(NUMLAY)=-B(NUMLAY)/XM
IF(NUMLAY.LE.1)GO TO 8
NUMLAY2=NUMLAY+1
NUMLAY1=NUMLAY-1
DO 9 L=1,NUMLAY1
L1=NUMLAY2-L
L2=L1-1
L3=L1-2
H=Z(L3)-Z(L2)
XMH=XM*H
ZZXM=ZZ(L1)*XM
HTAN=TANH(XMH)
CALL BJ(T,XM,U,RHO,EPSRHO,I,J,L2,B,OMP)
BL2=B(L2)
ZZNUM=ZZXM+BL2*HTAN
ZZDEN=ZZXM*HTAN+BL2
FRAC=BL2*ZZNUM/ZZDEN
ZZ(L2)=FRAC/XM
9 CONTINUE
Z0=ZZ(L2)
GO TO 7
8 ZZ=ZZ(NUMLAY)
7 CONTINUE

```

```

RETURN
END
SUBROUTINE GAUSS(XM,Z0,XIGR,Z,NUMLAY,T,U,RHO,
1 EPSRHO,I,J,B)

```

```

C SUBROUTINE GAUSS COMPUTES THE INTEGRAL OVER A RANGE OF
C EIGENVALUES AT A GIVEN TIME
DIMENSION T(50),U(5),RHO(5),EPSRHO(5),Z(5)
DIMENSION B(5)

```

```

DEL1=XM
CALL IYP(Z,Z0,NUMLAY,T,DEL1,U,RHO,EPSRHO,I,J,
1 B,OMP)

```

```

4010 FORMAT(3X,16HDIVISION BY ZERO)
XIGR=Z0
XIGI=0.

```

```

GO TO 33
WRITE(2,4020)DEL1,OMP,T(J),ZC

```

```

33 CONTINUE

```

```

4020 FORMAT(3X,2HM=,1E10.3,3X,2HF=,1E10.3,3X,2HT=,F10.3,3X,
12HA=,1E10.3)
RETURN

```

```

END

```

T-1879

```

SUBROUTINE ARTANH(X, ATANH)
C SUBROUTINE ARTANH COMPUTES THE HYPERBOLIC ARCTANGENT
CP=1.+X
CM=1.-X
ALOGCP=ALOG(CP)
ALOGCM=ALOG(CM)
ATANH=.5*(ALOGCP-ALOGCM)
GO TO 32
31 WRITE(2,5000)
5000 FORMAT(3X,12HLOG NEGATIVE)
32 CONTINUE
RETURN
END
SUBROUTINE DELTIME(XINTG, MAXTIME, T, NUMLAY)
C SUBROUTINE DELTIME COMPUTES THE DERIVATIVE OF THE IMPEDANCE
DIMENSION XINTG(50), T(50)
DIMENSION ZT(50), ZT1(50)
DO 4 J=1, MAXTIME
DELT=T(J+1)-T(J)
IF(NUMLAY.EQ.1) GO TO 1
ZT(J)=(XINTG(J+1)-XINTG(J))/DELT
GO TO 2
1 ZT1(J)=(XINTG(J+1)-XINTG(J))/DELT
2 CONTINUE
2000 FORMAT(3X,3HZT=,E10.3,3X,2HT=,F10.4)
IF(NUMLAY.GT.1) GO TO 3
RATIO=ZT(J)/ZT1(J)
WRITE(2,2001) RATIO, T(J)
3 CONTINUE
2001 FORMAT(3X,6HRATIO=,E10.3,3X,2HT=,F10.4)
4 CONTINUE
RETURN
END

```

T-1879

```

PROGRAM DATA(INPUT,OUTPUT,TAPE1=INPJ1,TAPE2)
DIMENSION DEX(200),DEY(200),DDBDT(200),ET(200)
DIMENSION DHDT(200),T(200),HX(200),Z(200),DZT(200)
DIMENSION U(5),RHO(5),EPSRHO(5),THICK(5),B(5)
DIMENSION XINTG(200),ZT1(200)

```

```

READ(1,*)J
READ(1,*)TURNS,AREA,R,AMP,NT
READ(1,*)VEX,VEY,VDBDT,VI,DCX,DCY
READ(1,*)(DEX(I),I=1,NT)
READ(1,*)(DEY(I),I=1,NT)
READ(1,*)(DDBDT(I),I=1,NT)

```

```

XMMAX=5.
XMMIN=1.E-09

```

```

C XMAX,XMMIN ARE THE MAXIMUM AND MINIMUM VALUES OVER WHICH THE
C INTEGRATION OF THE EIGENVALUES IS CARRIED OUT
INT=500

```

```

C INT REPRESENTS THE TOTAL NUMBER OF INTERVALS USED IN THE
C INTEGRATION OF THE EIGENVALUUES

```

```

NUMLAY=1
LXMIN=1

```

```

INTM=1
NULAY=NUMLAY-1
READ(1,*)(U(K),K=1,NUMLAY)

```

```

READ(1,*)(RHO(K),K=1,NUMLAY)
READ(1,*)(EPSRHO(K),K=1,NUMLAY)
READ(1,*)(THICK(K),K=1,NULAY)

```

```

WRITE(2,1000)J
WRITE(2,*)(U(K),K=1,NUMLAY)
WRITE(2,*)(RHO(K),K=1,NUMLAY)
WRITE(2,*)(EPSRHO(K),K=1,NUMLAY)
WRITE(2,*)(THICK(K),K=1,NULAY)

```

```

1000 FORMAT(3X,13HLINE-NUMBER ,I4)

```

```

WRITE(2,1001)TURNS,AREA,R,AMP,NT

```

```

1001 FORMAT(3X,2HN=,E10.3,3X,2HA=,E10.3,3X,2HR=,E10.3,3X,2HI=,
1E10.3,3X,7HPOINTS=,I4)

```

```

WRITE(2,1002)VEX,VEY,VDBDT,VI,DCX,DCY

```

```

1002 FORMAT(3X,4HVEX=,E10.3,3X,4HVEY=,E10.3,3X,6HVDBDT=,
1E10.3,3X,3HTI=,E10.3,3X,4HDCX=,E10.3,3X,4HDCY=,E10.3)

```

```

DO 1 I=1,NT

```

```

WRITE(2,1003)DEX(I),DEY(I),DDBDT(I)

```

```

1003 FORMAT(3X,4HDEX=,E10.3,3X,4HDEY=,E10.3,
13X,6HDDBDT=,E10.3)

```

```

1 CONTINUE

```

```

PI=3.14159

```

```

XMU=1.255E-05

```

```

HZ=0.0

```

```

AN=TURNS*AREA

```

```

PI2R=2.*PI*R

```

```

C1=AMP/PI2R

```

```

C2=C1**3

```

```

DO 2 I=1,NT

```

T-1879

```

EX=DEX(I)*JEX-DCX
EY=DEY(I)*VEY-DCY
IF(EX.EQ.0.0)GO TO 14
EYEX=EY/EX
THETA=ATAN(EYEX)
GO TO 12
14 THETA=PI/2.
12 CONTINUE
1008 FORMAT(3X,5HTHETA=,E10.3,3X,3HET=,E10.3)
ANDBDT=DDBDT(I)*VDBDT
DBDT=ANDBDT/AN
DHDT(I)=DBDT/XMU
T(I)=TI*I

EX2=EX*EX
EY2=EY*EY
EX2EY2=EX2+EY2
ET(I)=SORT(EX2EY2)
DA=DHDT(I)*TI
HZ=HZ+JA
IF(HZ.EQ.0.0)GO TO 6
C3=2.*C2/HZ
6 CONTINUE
HX(I)=SQRT(C3)
PITHET=PI/2.-THETA
PI2=PI/2.
IF(THETA.EQ.PI2)GO TO 17
H=HX(I)*COS(PITHET)
GO TO 15
17 H=HX(I)
15 CONTINUE
IF(H.EQ.0.0)GO TO 5
Z(I)=ET(I)/H
5 CONTINUE
IF(HX(I).EQ.0.0)GO TO 16
ZEY=EY/HX(I)
ZEX=ET(I)/HX(I)
16 CONTINUE
WRITE(2,1004)T(I),Z(I)
1004 FORMAT(3X,2HT=,E10.3,3X,2HZ=,E10.3)
1010 FORMAT(3X,4HZEY=,E10.3,3X,4HZEX=,E10.3)
2 CONTINUE
Z(1)=0.0
DO 3 I=1,NT
DZT(I)=(Z(I+1)-Z(I))/TI
IF(DZT(I).LT.2.)GO TO 18
GO TO 19
18 MAXTIME=I
GO TO 20
19 CONTINUE

```

T-1879

3 CONTINUE
20 CONTINUE

1005 FORMAT(3X,2HDT=,E10.3,3X,2HT=,E10.3)
CALL HAFSPAS(MAXTIME,NUMLAY,XMMAX,XMMIN,LXMIN,INT,INTM,
1T,U,RHO,EPSRHO,THICK,NT,ZT1)

DO 10 J=1,MAXTIME
RATIO=DZT(J)/ZT1(J)

10 WRITE(2,1006)RATIO,T(J)

1006 FORMAT(3X,2HR=,E10.3,3X,2HT=,E10.3)

11 CONTINUE
CALL EXIT

END

SUBROUTINE HAFSPAS(MAXTIME,NUMLAY,XMMAX,XMMIN,LXMIN,
1INT,INTM,T,U,RHO,EPSRHO,THICK,NT,ZT1)

C SUBROUTINE HAFSPAS COMPUTES THE DERIVATIVE OF THE IMPEDANCE OF AN
C INFINITE HALFSpace

DIMENSION T(200),U(5),RHO(5),EPSRHO(5),THICK(5)

DIMENSION B(5),XINTG(200),ZT1(200)

DO 30 M=1,INTM

DELXM=(XMMAX-XMMIN)/INT

DO 2 J=1,MAXTIME

CALL GAUSS(XMMIN,Z0,XIGR,THICK,NUMLAY,T,U,RHO,

1EPSRHO,I,J,B)

SUMIGR=XIGR*DELXM/2.

SUMIGI=XIGI*DELXM/2.

XM=XMMIN+DELXM

DO 1 I=1,INT

CALL GAUSS(XM,Z0,XIGR,THICK,NUMLAY,T,U,RHO,

1EPSRHO,I,J,B)

XIGR=XIGR*DELXM

SUMIGR=SUMIGR+XIGR

1000 FORMAT(2X,1E10.3)

XM=XM+DELXM

IF(XM.GT.XMMAX)GO TO 23

1 CONTINUE

23 CONTINUE

1002 FORMAT(1X,7HNUMINT=,I4)

XINTG(J)=SUMIGR

GO TO 13

WRITE(2,1007)T(J),SUMIGR

13 CONTINUE

1007 FORMAT(3X,2HT=,E10.4,3X,2HA=,E10.3)

2 CONTINUE

CALL DELTIME(XINTG,MAXTIME,T,ZT1)

INT=INT+LXMIN

30 CONTINUE

RETURN

END

SUBROUTINE BJ(T,XM,U,RHO,EPSRHO,I,J,K,B,CMP)

T-1879

```

C
C SUBROUTINE BJ COMPUTES EXPRESSION B(J), I.E. THE TIME
C FUNCTION FOR A GIVEN LAYER AT A GIVEN TIME AND GIVEN EIGENVALUE
DIMENSION T(50),U(5),RHO(5),EPSRHO(5)
DIMENSION B(5)
XMM=XM*XM
TAU=EPSRHO(K)*2.
C3=1./TAU
TTAU=TAU*TAU
VV=RHO(K)/(U(K)*EPSRHO(K))
V=SQRT(VV)
C1=1./TTAU
WW=XMM*VV+C1
W=SQRT(WW)
1001 FORMAT(2X,1E10,3)
TAUW=TAU*W
C2=1./TAUW
WT=T(J)*W
WMT=-WT
A=V*XM
TANHWT=TANH(WT)
S1=2.*TTAU*XMM*VV*TANHWT
S2=2.*TTAU*W*TANHWT
B(K)=-U(K)*S1/S2
GO TO 41
40 BETAM=-BETA
B(K)=-J(K)*A*EXP(BETAM)
41 CONTINUE
OMP=(-C3+W)/6.2331353
RETURN
END
SUBROUTINE IMP(THICK,ZI,NUMLAY,T,XM,U,RHO,EPSRHO,I,J,
1B,OMP)
DIMENSION T(200),U(5),RHO(5),EPSRHO(5),THICK(5)
DIMENSION ZZ(5),B(5)
THICK(0)=0.
CALL BJ(T,XM,U,RHO,EPSRHO,I,J,NUMLAY,B,OMP)
ZZ(NUMLAY)=-B(NUMLAY)/XM
IF(NUMLAY.LE.1)GO TO 3
NUMLAY2=NUMLAY+1
NUMLAY1=NUMLAY-1
DO 9 L=1,NUMLAY1
L1=NUMLAY2-L
L2=L1-1
L3=L1-2
H=THICK(L3)-THICK(L2)
XMH=XM*H
ZZXM=ZZ(L1)*XM
HTAN=TANH(XMH)
CALL BJ(T,XM,U,RHO,EPSRHO,I,J,L2,B,OMP)

```

```

BL2=B(L2)
ZZNUM=ZZXM+BL2*HTAN
ZZDEN=ZZXM*HTAN+BL2
FRAC=BL2*ZZNUM/ZZDEN
ZZ(L2)=FRAC/XM

```

```

9 CONTINUE
Z0=ZZ(L2)
GO TO 7

```

```

8 Z0=ZZ(NUMLAY)
7 CONTINUE
RETURN

```

```

END

```

```

SUBROUTINE GAUSS(XM,Z0,XIGR,THICK,NJMLAY,T,U,RHO,
1EPSRHO,I,J,B)

```

```

DIMENSION T(200),U(5),RHO(5),EPSRHO(5),THICK(5)
DIMENSION B(5)
DEL1=XM

```

```

CALL IMP(THICK,Z0,NUMLAY,T,DEL1,U,RHO,EPSRHO,I,J,
1B,OMP)

```

```

4010 FORMAT(3X,16HDIVISION BY ZERO)

```

```

XIGR=Z0
XIGI=0.
GO TO 33

```

```

WRITE(2,4020)DEL1,OMP,T(J),Z0

```

```

33 CONTINUE

```

```

4020 FORMAT(3X,2HM=,1E10,3,3X,2HF=,1E10,3,3X,2HT=,F10,3,3X,

```

```

12HA=,1E10.3)

```

```

RETURN
END

```

```

SUBROUTINE ARTANH(X,ATANH)

```

```

CP=1.+X
CM=1.-X

```

```

ALOGCP=ALOG(CP)
ALOGCM=ALOG(CM)
ATANH=.5*(ALOGCP-ALOGCM)

```

```

GO TO 32

```

```

31 WRITE(2,5000)

```

```

5000 FORMAT(3X,12HLOG NEGATIVE)

```

```

32 CONTINUE

```

```

RETURN
END

```

```

SUBROUTINE DELTIME(XINTG,MAXTIME,T,ZT1)

```

```

DIMENSION XINTG(200),T(200)
DIMENSION ZT1(200)

```

```

DO 4 J=1,MAXTIME
DELT=T(J+1)-T(J)
ZT1(J)=(XINTG(J+1)-XINTG(J))/DELT

```

```

2000 FORMAT(3X,3HZT=,E10.3,3X,2HT=,F10.4)

```

```

4 CONTINUE
RETURN

```

```

END

```

/list

LINE-NUMBER 4

29.

.000001256

100.001

.5

N=	.260E+02	A=	.578E+04	R=	.310E+05	I=	.290E+03	POINTS=	29	DCX=	0.	DCY=	0.
VEX=	.700E-05	VEY=	.680E-05	VDRDT=	.220E-06	TI=	.257E+00						
DEX=	.500E+00	DEY=	.500E+00	DDBDT=	.300E+00								
DEX=	.320E+01	DEY=	.160E+01	DDBDT=	.220E+01								
DEX=	.700E+01	DEY=	.270E+01	DDBDT=	.550E+01								
DEX=	.116E+02	DEY=	.390E+01	DDBDT=	.120E+02								
DEX=	.155E+02	DEY=	.480E+01	DDBDT=	.175E+02								
DEX=	.190E+02	DEY=	.600E+01	DDBDT=	.220E+02								
DEX=	.210E+02	DEY=	.670E+01	DDBDT=	.227E+02								
DEX=	.225E+02	DEY=	.730E+01	DDBDT=	.220E+02								
DEX=	.234E+02	DEY=	.760E+01	DDBDT=	.204E+02								
DEX=	.234E+02	DEY=	.750E+01	DDBDT=	.187E+02								
DEX=	.230E+02	DEY=	.740E+01	DDBDT=	.165E+02								
DEX=	.220E+02	DEY=	.730E+01	DDBDT=	.146E+02								
DEX=	.210E+02	DEY=	.670E+01	DDBDT=	.125E+02								
DEX=	.200E+02	DEY=	.640E+01	DDBDT=	.106E+02								
DEX=	.190E+02	DEY=	.590E+01	DDBDT=	.900E+01								
DEX=	.180E+02	DEY=	.560E+01	DDBDT=	.740E+01								
DEX=	.170E+02	DEY=	.540E+01	DDBDT=	.590E+01								
DEX=	.160E+02	DEY=	.509E+01	DDBDT=	.480E+01								
DEX=	.150E+02	DEY=	.500E+01	DDBDT=	.350E+01								
DEX=	.143E+02	DEY=	.470E+01	DDBDT=	.290E+01								
DEX=	.133E+02	DEY=	.450E+01	DDBDT=	.220E+01								
DEX=	.125E+02	DEY=	.430E+01	DDBDT=	.180E+01								
DEX=	.118E+02	DEY=	.409E+01	DDBDT=	.140E+01								
DEX=	.110E+02	DEY=	.400E+01	DDBDT=	.100E+01								
DEX=	.104E+02	DEY=	.380E+01	DDBDT=	.800E+00								
DEX=	.100E+02	DEY=	.360E+01	DDBDT=	.500E+00								
DEX=	.950E+01	DEY=	.340E+01	DDBDT=	.300E+00								
DEX=	.930E+01	DEY=	.330E+01	DDBDT=	.900E-01								

DEX= .900E+01 DDBDT= 0.

DEY= .320E+01

Z=

T=	.257E+00	Z=	.259E-04
T=	.514E+00	Z=	.607E-03
T=	.771E+00	Z=	.284E-02
T=	.103E+01	Z=	.829E-02
T=	.129E+01	Z=	.162E-01
T=	.154E+01	Z=	.247E-01
T=	.180E+01	Z=	.318E-01
T=	.206E+01	Z=	.378E-01
T=	.231E+01	Z=	.429E-01
T=	.257E+01	Z=	.466E-01
T=	.283E+01	Z=	.482E-01
T=	.309E+01	Z=	.469E-01
T=	.334E+01	Z=	.479E-01
T=	.360E+01	Z=	.468E-01
T=	.386E+01	Z=	.466E-01
T=	.411E+01	Z=	.449E-01
T=	.437E+01	Z=	.422E-01
T=	.463E+01	Z=	.401E-01
T=	.488E+01	Z=	.365E-01
T=	.514E+01	Z=	.354E-01
T=	.540E+01	Z=	.323E-01
T=	.566E+01	Z=	.301E-01
T=	.591E+01	Z=	.283E-01
T=	.617E+01	Z=	.255E-01
T=	.643E+01	Z=	.240E-01
T=	.668E+01	Z=	.234E-01
T=	.694E+01	Z=	.223E-01
T=	.720E+01	Z=	.220E-01
T=	.746E+01	Z=	.213E-01
R=	.150E+05	T=	.257E+00
R=	.553E+05	T=	.514E+00
R=	.135E+06	T=	.771E+00
R=	.196E+06	T=	.103E+01
R=	.208E+06	T=	.129E+01

R=	.176E+06	T=	.154E+01
R=	.149E+06	T=	.180E+01
R=	.127E+06	T=	.206E+01
R=	.894E+05	T=	.231E+01
R=	.400E+05	T=	.257E+01
R=	.277E+04	T=	.283E+01

list
LINE-NUMBER 6

54.
.000001256
100.001
.5

N=	.260E+02	A=	.581E+04	R=	.300E+05	I=	.290E+03	POINTS=	54.	DCX=	.700E-05	DCY=	0.
VEY=	.230E-05	VEY=	.732E-06	VDRDT=	.230E-06	TI=	.243E+00						
DEX=	.400E+01	DEY=	.200E+01	DRDT=	.300E+01								
DEX=	.650E+01	DEY=	.500E+01	DRDT=	.600E+01								
DEX=	.890E+01	DEY=	.800E+01	DRDT=	.110E+02								
DEX=	.112E+02	DEY=	.100E+02	DRDT=	.170E+02								
DEX=	.130E+02	DEY=	.123E+02	DRDT=	.225E+02								
DEX=	.140E+02	DEY=	.145E+02	DRDT=	.270E+02								
DEX=	.150E+02	DEY=	.170E+02	DRDT=	.296E+02								
DEX=	.159E+02	DEY=	.190E+02	DRDT=	.307E+02								
DEX=	.160E+02	DEY=	.210E+02	DRDT=	.309E+02								
DEX=	.160E+02	DEY=	.225E+02	DRDT=	.302E+02								
DEX=	.160E+02	DEY=	.240E+02	DRDT=	.290E+02								
DEX=	.160E+02	DEY=	.253E+02	DRDT=	.280E+02								
DEX=	.160E+02	DEY=	.268E+02	DRDT=	.264E+02								
DEX=	.159E+02	DEY=	.276E+02	DRDT=	.250E+02								
DEX=	.157E+02	DEY=	.280E+02	DRDT=	.235E+02								
DEX=	.155E+02	DEY=	.283E+02	DRDT=	.218E+02								
DEX=	.153E+02	DEY=	.284E+02	DRDT=	.203E+02								
DEX=	.152E+02	DEY=	.282E+02	DRDT=	.187E+02								
DEX=	.151E+02	DEY=	.280E+02	DRDT=	.173E+02								
DEX=	.150E+02	DEY=	.279E+02	DRDT=	.160E+02								
DEX=	.149E+02	DEY=	.277E+02	DRDT=	.148E+02								
DEX=	.146E+02	DEY=	.274E+02	DRDT=	.133E+02								
DEX=	.144E+02	DEY=	.270E+02	DRDT=	.120E+02								
DEX=	.142E+02	DEY=	.267E+02	DRDT=	.114E+02								
DEX=	.140E+02	DEY=	.260E+02	DRDT=	.105E+02								
DEX=	.139E+02	DEY=	.254E+02	DRDT=	.980E+01								
DEX=	.137E+02	DEY=	.247E+02	DRDT=	.900E+01								
DEX=	.135E+02	DEY=	.240E+02	DRDT=	.840E+01								

DEX=	.133E+02	DEY=	.234E+02	DDBDI=	.780E+01
DEX=	.130E+02	DEY=	.226E+02	DDBDI=	.720E+01
DEX=	.129E+02	DEY=	.215E+02	DDBDI=	.670E+01
DEX=	.127E+02	DEY=	.207E+02	DDBDI=	.600E+01
DEX=	.125E+02	DEY=	.200E+02	DDBDI=	.560E+01
DEX=	.123E+02	DEY=	.190E+02	DDBDI=	.500E+01
DEX=	.120E+02	DEY=	.180E+02	DDBDI=	.480E+01
DEX=	.119E+02	DEY=	.170E+02	DDBDI=	.420E+01
DEX=	.117E+02	DEY=	.160E+02	DDBDI=	.370E+01
DEX=	.115E+02	DEY=	.150E+02	DDBDI=	.340E+01
DEX=	.113E+02	DEY=	.140E+02	DDBDI=	.290E+01
DEX=	.112E+02	DEY=	.130E+02	DDBDI=	.270E+01
DEX=	.110E+02	DEY=	.120E+02	DDBDI=	.230E+01
DEX=	.108E+02	DEY=	.110E+02	DDBDI=	.200E+01
DEX=	.105E+02	DEY=	.100E+02	DDBDI=	.170E+01
DEX=	.103E+02	DEY=	.950E+01	DDBDI=	.150E+01
DEX=	.101E+02	DEY=	.860E+01	DDBDI=	.120E+01
DEX=	.100E+02	DEY=	.770E+01	DDBDI=	.100E+01
DEX=	.930E+01	DEY=	.700E+01	DDBDI=	.800E+00
DEX=	.950E+01	DEY=	.609E+01	DDBDI=	.600E+00
DEX=	.930E+01	DEY=	.520E+01	DDBDI=	.500E+00
DEX=	.909E+01	DEY=	.440E+01	DDBDI=	.400E+00
DEX=	.900E+01	DEY=	.360E+01	DDBDI=	.300E+00
DEX=	.880E+01	DEY=	.270E+01	DDBDI=	.200E+00
DEX=	.850E+01	DEY=	.180E+01	DDBDI=	.990E-01
DEX=	.830E+01	DEY=	.100E+01	DDBDI=	0.
I=	.243E+00	Z=	.525E-04		
T=	.485E+00	Z=	.399E-03		
T=	.728E+00	Z=	.105E-02		
T=	.970E+00	Z=	.214E-02		
T=	.121E+01	Z=	.330E-02		
T=	.146E+01	Z=	.416E-02		
T=	.170E+01	Z=	.501E-02		
T=	.194E+01	Z=	.591E-02		
T=	.218E+01	Z=	.620E-02		
T=	.243E+01	Z=	.645E-02		

T=	.267E+01	Z=	.666E-02
T=	.291E+01	Z=	.688E-02
T=	.315E+01	Z=	.704E-02
T=	.340E+01	Z=	.718E-02
T=	.364E+01	Z=	.724E-02
T=	.388E+01	Z=	.729E-02
T=	.412E+01	Z=	.733E-02
T=	.437E+01	Z=	.744E-02
T=	.461E+01	Z=	.753E-02
T=	.485E+01	Z=	.761E-02
T=	.509E+01	Z=	.767E-02
T=	.534E+01	Z=	.755E-02
T=	.558E+01	Z=	.751E-02
T=	.582E+01	Z=	.745E-02
T=	.606E+01	Z=	.742E-02
T=	.631E+01	Z=	.745E-02
T=	.655E+01	Z=	.740E-02
T=	.679E+01	Z=	.734E-02
T=	.703E+01	Z=	.727E-02
T=	.728E+01	Z=	.711E-02
T=	.752E+01	Z=	.718E-02
T=	.776E+01	Z=	.712E-02
T=	.800E+01	Z=	.704E-02
T=	.825E+01	Z=	.700E-02
T=	.849E+01	Z=	.686E-02
T=	.873E+01	Z=	.695E-02
T=	.897E+01	Z=	.694E-02
T=	.922E+01	Z=	.694E-02
T=	.946E+01	Z=	.696E-02
T=	.970E+01	Z=	.714E-02
T=	.994E+01	Z=	.721E-02
T=	1.02E+02	Z=	.733E-02
T=	1.04E+02	Z=	.733E-02
T=	1.07E+02	Z=	.726E-02
T=	1.09E+02	Z=	.742E-02
T=	1.12E+02	Z=	.790E-02

6-4

T=	.114E+02	Z=	.809E-02
T=	.116E+02	Z=	.835E-02
T=	.119E+02	Z=	.902E-02
T=	.121E+02	Z=	.981E-02
T=	.124E+02	Z=	.115E-01
T=	.126E+02	Z=	.141E-01
T=	.129E+02	Z=	.187E-01
T=	.131E+02	Z=	.311E-01
R=	.105E+05	T=	.243E+00
R=	.170E+05	T=	.485E+00
R=	.287E+05	T=	.728E+00
R=	.303E+05	T=	.970E+00
R=	.227E+05	T=	.121E+01
R=	.223E+05	T=	.146E+01
R=	.235E+05	T=	.170E+01
R=	.746E+04	T=	.194E+01
R=	.665E+04	T=	.218E+01
R=	.558E+04	T=	.243E+01
R=	.557E+04	T=	.267E+01
R=	.426E+04	T=	.291E+01
R=	.360E+04	T=	.315E+01
R=	.182E+04	T=	.340E+01
R=	.124E+04	T=	.364E+01
R=	.982E+03	T=	.388E+01
R=	.298E+04	T=	.412E+01
R=	.225E+04	T=	.437E+01
R=	.201E+04	T=	.461E+01
R=	.161E+04	T=	.485E+01
R=	.144E+03	T=	.509E+01

List

LINE-NUMBER 9

23.
.000001256
10.001
.1001

	A=	.581E+04	R=	.315E+05	I=	.290E+03	POINTS=	23	DCX=	.380E-05	DCY=	.640E-0
DEX=	.260E+02	VEY=	.270E-06	VDBDT=	.270E-06	TI=	.590E-01					
DEX=	.857E-06	DEY=	.240E+01	DDBDT=	.170E+02							
DEX=	.450E+01	DEY=	.680E+01	DDBDT=	.305E+02							
DEX=	.113E+02	DEY=	.125E+02	DDBDT=	.345E+02							
DEX=	.190E+02	DEY=	.190E+02	DDBDT=	.330E+02							
DEX=	.260E+02	DEY=	.255E+02	DDBDT=	.295E+02							
DEX=	.315E+02	DEY=	.320E+02	DDBDT=	.245E+02							
DEX=	.355E+02	DEY=	.370E+02	DDBDT=	.200E+02							
DEX=	.380E+02	DEY=	.420E+02	DDBDT=	.170E+02							
DEX=	.390E+02	DEY=	.465E+02	DDBDT=	.140E+02							
DEX=	.391E+02	DEY=	.500E+02	DDBDT=	.120E+02							
DEX=	.390E+02	DEY=	.522E+02	DDBDT=	.100E+02							
DEX=	.384E+02	DEY=	.542E+02	DDBDT=	.800E+01							
DEX=	.373E+02	DEY=	.555E+02	DDBDT=	.550E+01							
DEX=	.360E+02	DEY=	.565E+02	DDBDT=	.480E+01							
DEX=	.350E+02	DEY=	.568E+02	DDBDT=	.400E+01							
DEX=	.330E+02	DEY=	.567E+02	DDBDT=	.300E+01							
DEX=	.320E+02	DEY=	.565E+02	DDBDT=	.240E+01							
DEX=	.307E+02	DEY=	.555E+02	DDBDT=	.180E+01							
DEX=	.293E+02	DEY=	.550E+02	DDBDT=	.140E+01							
DEX=	.280E+02	DEY=	.538E+02	DDBDT=	.120E+01							
DEX=	.270E+02	DEY=										

9-1

9-2

DEX=	.260E+02	DEY=	.520E+02	DDRDI=	.800E+00
DEX=	.250E+02	DEY=	.505E+02	DDBDI=	.500E+00
DEX=	.245E+02	DEY=	.490E+02	DDRDI=	0.
T=	.590E-01	Z=	.613E-05		
T=	.118E+00	Z=	.759E-03		
T=	.177E+00	Z=	.198E-02		
T=	.236E+00	Z=	.316E-02		
T=	.295E+00	Z=	.406E-02		
T=	.354E+00	Z=	.459E-02		
T=	.413E+00	Z=	.492E-02		
T=	.472E+00	Z=	.486E-02		
T=	.531E+00	Z=	.466E-02		
T=	.590E+00	Z=	.451E-02		
T=	.649E+00	Z=	.435E-02		
T=	.708E+00	Z=	.408E-02		
T=	.767E+00	Z=	.382E-02		
T=	.826E+00	Z=	.363E-02		
T=	.885E+00	Z=	.330E-02		
T=	.944E+00	Z=	.315E-02		
T=	.100E+01	Z=	.296E-02		
T=	.106E+01	Z=	.277E-02		
T=	.112E+01	Z=	.259E-02		
T=	.118E+01	Z=	.247E-02		
T=	.124E+01	Z=	.236E-02		
T=	.130E+01	Z=	.224E-02		
T=	.136E+01	Z=	.219E-02		
R=	.818E+04	T=	.590E-01		
R=	.131E+05	T=	.118E+00		
R=	.127E+05	T=	.177E+00		
R=	.972E+04	T=	.236E+00		
R=	.572E+04	T=	.295E+00		
R=	.353E+04	T=	.354E+00		
R=	.820E+02	T=	.413E+00		

```

/list
25 3
.05 .5
.000001256 .000001256 .000001256
10. .5 100.
.1 .5 .1
235. 500.
RATIO= .194E+01 T= .0500
RATIO= .327E+01 T= .0550
RATIO= .695E+01 T= .0605
RATIO= .180E+02 T= .0666
RATIO= .548E+02 T= .0732
RATIO= .189E+03 T= .0805
RATIO= .724E+03 T= .0886
RATIO= .284E+04 T= .0974
RATIO= .856E+04 T= .1072
RATIO= .140E+05 T= .1179
RATIO= .151E+05 T= .1297
RATIO= .146E+05 T= .1427
RATIO= .137E+05 T= .1569
RATIO= .126E+05 T= .1726
RATIO= .113E+05 T= .1899
RATIO= .100E+05 T= .2089
RATIO= .866E+04 T= .2297
RATIO= .732E+04 T= .2527
RATIO= .606E+04 T= .2780
RATIO= .488E+04 T= .3058
RATIO= .383E+04 T= .3364
RATIO= .293E+04 T= .3700
RATIO= .217E+04 T= .4070
RATIO= .156E+04 T= .4477
RATIO= .100E+01 T= .4925

```

REFERENCES

- Bear, H. S., 1962, Differential equations: Reading, Mass., Addison-Wesley Publishing Comp., Inc., 207 p.
- Churchill, R. V., 1960, Complex variables and applications: New York, N.Y., McGraw-Hill Book Co., 297 p.
- Churchill, R. V., 1963, Fourier series and boundary value problems: New York, N.Y., McGraw-Hill Book Co., 248 p.
- Grant, F. S., and West, G. F., 1965, Interpretation theory in applied geophysics: New York, N.Y., McGraw-Hill Book Co., 584 p.
- Jackson, D., 1961, Fourier series and orthogonal polynomials: The Carus Mathematical Monographs, No. 6, The mathematical Association of America, 234 p.
- Keller, G. V., and Frischknecht, F. C., 1966, Electrical methods in geophysical prospecting: New York, N.Y., Pergamon Press, Inc., 519 p.
- Lienert, B., 1976, High electrical conductivities in the lower crust of the northwestern Basin and Range; an application of inverse theory to a controlled source deep magnetic sounding experiment: The OAR and CSM Conference on the Nature and Physical Properties of the crust, Vail, Colorado
- Morse, P. M., and Feshbach, H., 1953, Methods of theoretical physics: New York, N.Y., McGraw-Hill Book Co., 520 p.
- Papoulis, A., 1962, The Fourier integral and its applications: New York, N.Y., McGraw-Hill Book Co., 318 p.
- Stratton, J. A., 1941, Electromagnetic theory: New York, N.Y., McGraw-Hill Book Co., 615 p.
- _____, 1967, Mining geophysics: Tulsa, Oklahoma, The Society of Exploration Geophysicists, 708 p.
- Tikhonov, A. N., and Samarskii, A.A., 1963, Equations of mathematical physics: Oxford, Pergamon Press, 432 p.